Matching Network Elimination in Broadband Rectennas for High-Efficiency Wireless Power Transfer and Energy Harvesting

Chaoyun Song, Yi Huang, *Senior Member, IEEE*, Jiafeng Zhou, Paul Carter, Sheng Yuan, Qian Xu, and Zhouxiang Fei

***Abstract*—Impedance matching networks for nonlinear devices such as amplifiers and rectifiers are normally very challenging to design, particularly for broadband and multiband devices. A novel design concept for a broadband high-efficiency rectenna without using matching networks is presented in this paper for the first time. An off-center-fed dipole antenna with relatively high input impedance over a wide frequency band is proposed. The antenna impedance can be tuned to the desired value and directly provides a complex conjugate match to the impedance of a rectifier. The received RF power by the antenna can be delivered to the rectifier efficiently without using impedance matching networks; thus, the proposed rectenna is of a simple structure, low cost, and compact size. In addition, the rectenna can work well under different operating conditions and using different types of rectifying diodes. A rectenna has been designed and made based on this concept. The measured results show that the rectenna is of high power conversion efficiency (more than 60%) in two wide bands, which are 0.9–1.1 and 1.8–2.5 GHz, for mobile, Wi-Fi, and ISM bands. Moreover, by using different diodes, the rectenna can maintain its wide bandwidth and high efficiency over a wide range of input power levels (from 0 to 23 dBm) and load values (from 200 to 2000 Ω). It is, therefore, suitable for high-efficiency wireless power transfer or energy harvesting applications. The proposed rectenna is general and simple in structure without the need for a matching network hence is of great significance for many applications.**

***Index Terms*—Broadband rectennas, impedance matching networks, off-center-fed dipole (OCFD), wireless energy harvesting (WEH), wireless power transmission.**

Manuscript received July 5, 2016; revised October 17, 2016 and November 14, 2016; accepted December 3, 2016. This work was supported in part by the Engineering and Physical Sciences Research Council, U.K., and in part by Aeternum LLC. *(Corresponding Author: Yi Huang.)*

C. Song, Y. Huang, J. Zhou, S. Yuan, and Z. Fei are with the Department of Electrical Engineering and Electronics, University of Liverpool, Liverpool, L69 3GJ, U.K. (e-mail: sgcsong2@liv.ac.uk; Yi.Huang@liv.ac.uk; zhouj@liverpool.ac.uk; sgsyuan@liverpool.ac.uk; zf1g12@liverpool.ac.uk).

P. Carter is with Global Wireless Solutions, Inc., Dulles, VA 20166 USA (e-mail: pcarter@gwsolutions.com).

Q. Xu is with the College of Electronic and Information Engineering, Nanjing University of Aeronautics and Astronautics, Nanjing 211106, China (e-mail: emxu@foxmail.com).

Color versions of one or more of the figures in this paper are available online at http://ieeexplore.ieee.org

Digital Object Identifier 10.1109/TIE.2016.2645505

I. Introduction

IMPEDANCE matching is a basic but crucial concept in electronics and electrical engineering, since it can maximize the power transfer from a source to a load or minimize the signal reflection from a load. In the wireless industry today, there have been many devices (such as oscillators, inverters, amplifiers, rectifiers, power dividers, boost converters) and systems that have a high demand for impedance matching networks. A number of techniques for the network design have been reported [1]–[6]. Among them, rectifiers and power amplifiers (PAs) normally utilize nonlinear elements such as diodes and transistors in the circuits. Hence their input impedance varies with the frequency, input power, and load impedance. The impedance matching networks for such nonlinear circuits become very challenging to design.

Wireless power transfer (WPT) and wireless energy harvesting (WEH) have attracted significant attention in the past few years [7]–[10]. In both radiative and inductive wireless power transmissions, the rectifiers are a vital device for converting ac or RF power to dc power, while impedance matching networks are required to achieve high conversion efficiency [9].

A rectifying antenna (*rectenna*) is one of the most popular devices for WPT and WEH applications, and much progress has been made [11]–[19]. Multiband and broadband rectennas [15]–[19] can receive or harvest RF power from different sources and from different channels simultaneously; thus, they outperform the conventional single band rectennas [11]–[14] in terms of overall conversion efficiency as well as total output power. However, the design of the impedance matching network for broadband or multiband rectennas is very challenging, and the structure of the matching network is relatively complex which may increase the cost and loss, and also introduce errors in manufacturing.

Some techniques such as resistance compression networks and frequency selective networks have been developed to reduce the nonlinear effects of the rectenna [20]–[24] so that the performance can be maintained under different operating conditions. But, they all require introduction of further circuit components in the matching network which increases the complexity of the overall design. Using more components could increase the loss and decrease the overall efficiency. A need exists, therefore, for rectennas comprising simple structures

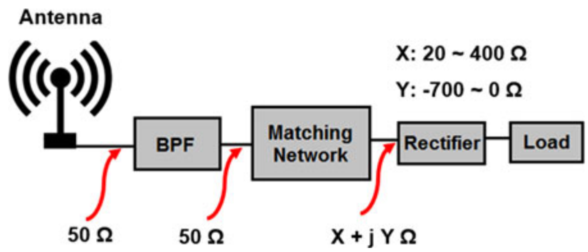

Fig. 1. Configuration of a conventional rectifying antenna system with impedance matching networks.

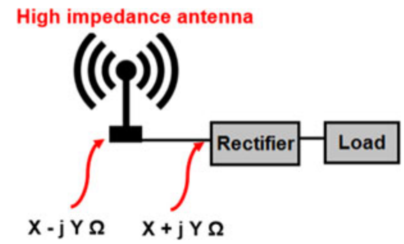

Fig. 2. Configuration of the proposed rectifying antenna without using impedance matching networks.

with competitive performance. It is desirable that the impedance matching network is eliminated or simplified, but the received RF power at different frequency bands can still be delivered to the rectifier with high RF–dc conversion efficiency.

Some designs use a standard antenna with 50 Ω impedance to match with a rectifier. Thus, either the operating bandwidth is narrow [25], or the conversion efficiency over the broadband is low, typically $<20\%$ [26]. So far there are no available designs without matching networks, that can produce high conversion efficiency over a wide frequency band, and there are no available approaches that can tune the antenna impedance to the desired value to match with the impedance of the rectifier.

In this paper, we propose a novel methodology for a high-efficiency broadband rectenna without the use of a matching network. The concept and operating mechanism are introduced in Section II. The approaches for designing a broadband high impedance antenna are discussed in Section III. The rectenna integration that can eliminate the use of matching networks is shown in Section IV. The experimental validations and measurements of a fabricated rectenna example are shown in Section V. To the best of our knowledge, the proposed design is the first broadband rectenna without using matching networks and achieves good performance; that is, high RF–dc conversion efficiency and improved linearity over a wide frequency band, a range of input power levels, and load impedance.

II. Novelty of This Work

A conventional rectifying antenna system, as shown in Fig. 1, normally consists of five different parts.

1) First of all, a receiving antenna is normally configured to receive signals from a predetermined source (WPT) or to receive random signals in the ambient environment (WEH). The input impedance of the antenna is usually matched to standard 50 Ω.
2) Secondly, a band pass filter is required to reject the higher order harmonic signals generated by the rectifier, since the signals could be radiated by the antenna which might reduce the overall conversion efficiency and cause interference. In some cases, the filter can either be embedded with the antenna to produce a filtering-antenna structure [27] or be integrated with the impedance matching network [18] to make the complete design simple and compact.
3) Thirdly, in order to match the complex impedance of the rectifier to a resistive port (e.g., 50 Ω), an impedance matching network is usually placed between the antenna and the rectifier. Thus, the power of the received signals could be fully delivered to the rectifier.
4) Fourthly, for rectification, a rectifier is configured to convert RF power to dc power. The input impedance of the rectifier varies in a wide range of values and the impedance is very sensitive to the variation of frequency, input power, and load impedance.
5) Finally, a resistive load is necessary for applications. The load could typically be a resistor, a dc-to-dc boost converter for realizing a higher output voltage, or a super capacitor to store energy.

In previous studies [18], [24], the impedance of the rectifier was analyzed under different operating conditions such as a wide frequency range (e.g., 0.5–3 GHz), a range of input powers (e.g., –40 to 0 dBm), and a wide load impedance range (e.g., 1–100 kΩ). It is concluded that the input impedance of the rectifier varies significantly (20–400 Ω for the real part, 0 to –700 Ω for the imaginary part) over these operating conditions. Furthermore, due to nonlinearity, the impedance of the rectifier would also vary with different types of rectifying diodes and different circuit topologies. However, as shown in Fig. 1, most parts are connected by using a 50 Ω port in the conventional rectenna configuration. Therefore, the design of the impedance matching network is usually the most challenging part, particularly in multiband or broadband rectennas. Thus, in previous work [19], [24], the structures of the impedance matching networks were complex for broadband and multiband rectennas, while the number of circuit components used in the matching network was very large (i.e., more than 25 elements) to reduce the nonlinear effects and produce a consistent performance. Consequently, the complex matching networks may introduce errors from manufacture, increase the cost and loss, and create additional problems.

In this work, we propose a novel method for broadband or multiband rectenna designs. The aim is to eliminate the need for impedance matching networks and to improve the overall performance of the rectenna. As shown in Fig. 2, the proposed new configuration only consists of three parts, wherein the antenna is changed to a special high impedance antenna which is very different from conventional ones. The impedance of the antenna is around 200–300 Ω for the real part and 0–300 Ω for the imaginary part in desired frequency band. The value of the antenna impedance ($X - jY$) may directly conjugate match with the input impedance of a specific rectifier ($X + jY$) within the desired frequency range but mismatch at other frequencies

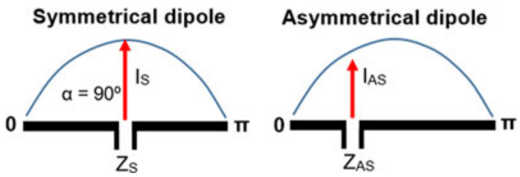

Fig. 3. Half-wavelength center-fed symmetrical dipole and the off-center-fed asymmetrical dipole.

TABLE I
SIMULATED INPUT IMPEDANCE OF THE OFF-CENTER-FED DIPOLE

Long arm (mm)	Short arm (mm)	Real part at f_0 (Ω)	Imaginary part at f_0 (Ω)
90	10	320	–213
80	20	165	–30
70	30	102	–0.8
60	40	79	5.6
50	50	73	6.4

(to produce a filtering response), as depicted in Fig. 2. Thus, a matching network can be eliminated and the proposed rectenna can offer high conversion efficiency over a broad bandwidth. Moreover, since both the rectifier and the antenna are of relatively high input impedance, the effects on the reflection coefficient (S_{11}) of the rectenna caused by the impedance variation of the nonlinear elements (rectifying diodes) may not be very significant. Therefore, compared with the conventional 50 Ω (low impedance) matching system, the nonlinear effects of the rectenna can be significantly reduced by using this new configuration. The rectenna may have a good performance in a range of operating conditions such as different input power levels, different load values, or even different types of rectifying diodes. In addition, the proposed rectenna configuration can reduce the total cost and avoid fabrication errors due to its very simple structure.

III. HIGH IMPEDANCE ANTENNA DESIGN

A. Off-Center-Fed Dipole Theory

There have been various types of high impedance antenna reported in the literature [28], [29], but none of them can provide a constantly high impedance over a wide frequency range which is very important for realizing the proposed broadband high-efficiency rectenna. There are no available approaches that can tune the antenna impedance over a wide frequency band to the desired values. Consequently, if these high impedance antennas were used without matching networks, the bandwidth of the rectenna could become very narrow.

Here, we propose a broadband high impedance antenna, the off-center-fed dipole (OCFD) antenna.

As depicted in Fig. 3, the OCFD antenna is different from a conventional center-fed symmetrical dipole antenna, where the two dipole arms are asymmetrical and have unequal lengths. The typical application of the OCFD is to realize a multiband antenna, since the resonant center-fed d has its fundamental frequency at f_0 and harmonics at $3\,f_0$, $5\,f_0$, $7\,f_0$, and so on. While the OCFD can resonate at f_0, $2\,f_0$, $4\,f_0$, and $8\,f_0$ by offsetting the feed by λ/4 from the center [30]. Such OCFDs are very popular in the amateur radio community. Recently, some researchers used the OCFD to create a 90° phase delay and generate circular polarization radiation field for the antenna [31]. But, one of the major problems of the OCFD is that the radiation resistance of the antenna could be very high; thus, it is required to use a 4:1 or 6:1 balun transformer to convert the impedance to the feeding port 50 Ω resistance [32]. This is a disadvantage for most of those applications using OCFDs (in a conventional 50 Ω feed system), but we may take advantage of this feature in the proposed rectenna design. The OCFD antenna may be well matched to a rectifier without using matching networks since the rectifiers are normally of high input impedance as well. We assume a half-wavelength center-fed dipole and an OCFD having the same total length and radiating the same power, as shown in Fig. 3. The currents at the feed points for the symmetrical and asymmetrical dipoles are I_S and I_{AS}, respectively. From [38], the relationship between the currents can be expressed as

$$I_{\mathrm{AS}} = I_S \sin\alpha \tag{1}$$

where α is the measured angle from one end in electrical degrees (between 0 and π as shown in Fig. 3). Thus, the power radiated by both antennas can be calculated as

$$P_S = I_S^2 R_S \tag{2}$$

$$P_{\mathrm{AS}} = I_{\mathrm{AS}}^2 R_{\mathrm{AS}} \tag{3}$$

where R_S and R_{AS} are the radiation resistances of the center-fed dipole and the OCFD, respectively. Since we have assumed $P_S = P_{\mathrm{AS}}$, thus we can obtain

$$\frac{R_S}{R_{\mathrm{AS}}} = \frac{I_{\mathrm{AS}}^2}{I_S^2}. \tag{4}$$

Using (1), the relationship between the radiation resistances R_S and R_{AS} can be written as

$$R_S = \frac{R_{\mathrm{AS}}}{(\sin\alpha)^2}. \tag{5}$$

Thus, when $\alpha = 90°$ or (π/2), the dipole is center-fed since $\sin\alpha = 1$ and $R_S = R_{\mathrm{AS}}$. It is demonstrated that the value of R_{AS} is always larger than the value of R_{S} if the dipole is off-center-fed. In addition, we could tune the radiation resistance of the OCFD to a desired value by changing the value of $\sin\alpha$ (position of the feed point).

In order to gain a better understanding, we study a simple OCFD antenna in free space with the aid of the CST software. Assume that the arms of the dipole are made by perfect electric conductor wires with a diameter of 1 mm. The total length of the OCFD is 100 mm while the feeding port separation is 1 mm. If the antenna is considered as a typical half-wavelength dipole, then the fundamental frequency should be about 1.5 GHz. The computed real part and imaginary part of the input impedance of the OCFD at 1.5 GHz are given in Table I for different feed locations. As can be seen from the table, the radiation resistance of the dipole is 73 Ω when the two arms have the same length. By changing the feed position, the radiation resistance can be

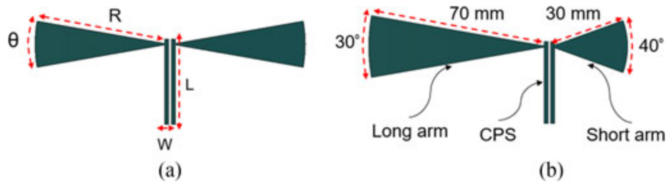

Fig. 4. (a) The broadband center-fed symmetrical dipole antenna. (b) The broadband off-center-fed dipole antenna.

increased where the value is about 320 Ω for the long arm being 90 mm and the short arm being 10 mm. Compared with the impedance of a symmetrical dipole (73 Ω), the OCFD has increased the impedance value up to 4.4 times. The imaginary part of the input impedance is around 0–6 Ω and the ratio of the long arm over the short arm is less than 7/3. Therefore, if the symmetrical dipole is of a broad bandwidth, the OCFD may produce constantly high impedance over the bandwidth of interest.

B. Broadband OCFD Antenna Design

A broadband center-fed symmetrical dipole is proposed as the starting point to design a broadband OCFD antenna. As shown in Fig. 4(a), the arms of the dipole are shaped as radial (bowtie) stubs to broaden the frequency bandwidth. The bowtie dipole antenna is a planar version of a biconical antenna. From [36], the characteristic impedance (Z_k) of an infinite biconical antenna is given by

$$Z_k = 120 \text{ In } \cot(\theta/4) \tag{6}$$

where θ is the cone angle. Then, the input impedance (Z_i) of the biconical antenna with a finite length can be written as

$$Z_i = Z_k \frac{Z_k + jZ_m \tan \beta l}{Z_m + jZ_K \tan \beta l} \tag{7}$$

where $\beta = 2\pi/\lambda$ (λ is the wavelength), $l =$ cone length, and $Z_m = R_m + j\,X_m$. While the values of R_m and X_m are given by Schellkunoff [37] for a thin biconical antenna ($\theta < 5°$). As indicated in [36], the VSWR of the biconical antenna can be less than 2 over a 2:1 bandwidth. Meanwhile, the input impedance of the bowtie dipole is similar to that of the biconical antenna, where the value of the impedance is a function of frequency, length of the arm (R), and cone angle (θ).

The aforementioned theories could be utilized to predict the initial performance (such as the frequency bandwidth) of this broadband antenna with a given dimension. But the actual performance might be varied in the simulation and measurement due to the practical configuration of the antenna (e.g., effects of PCB and feed). Therefore, in order to maintain the antenna performance, the major design parameters of the antenna should be further tuned using the software. As a design guide, the parametric effects (values of the R and θ) on the frequency bandwidth of the bowtie dipole [as shown in Fig. 4(a)] are studied. If the antenna is printed on a Rogers RT6002 board with a relative permittivity of 2.94 and a thickness of 1.52 mm, it is fed by a pair of coplanar striplines (CPS) where the length (L) of each strip is 32 mm and the width (W) is 1.5 mm. The gap between the CPS is 1 mm. The antenna is modeled using the CST software. The simulated frequency bandwidth (for VSWR <2 with 50 Ω port) of the bowtie dipole is shown in Table II for different cone angles and lengths of the arm.

From the results in Table II, it can be seen that the bowtie symmetrical dipole is indeed of a broad bandwidth. Moreover, the antenna could have a larger frequency bandwidth for larger cone angles, and have a lower resonant frequency band for larger dimensions (length of the arm). In this work, we select $R = 50$ mm and $\theta = 30°$ as an example, since the frequency band (from 1.75 to 2.17 GHz) has covered some popular mobile frequency bands such as the GSM1800 and UMTS2100. Hence, the arms of the symmetrical bowtie dipole have a radius of 50 mm and an angle of 30° for the radial stub structure. The maximum total length of the complete dipole antenna is about 100 mm.

To design the OCFD, the length of the longer arm is increased to 70 mm while the length of the shorter arm is, therefore, reduced to 30 mm. In addition, in order to enhance asymmetry between the arms, the circumference angle of the shorter arm is increased to 40°. The total length of the dipole is still of around 100 mm, as shown in Fig. 4(b). But the ratio of the long arm to the short arm has been changed from 5/5 to 7/3. In this scenario, the real part of the impedance over the frequency band may be increased while the imaginary part could be maintained over the resonant frequency band (as discussed in Table I). Fig. 5 shows the simulated real part of the input impedance of the symmetrical dipole and the OCFD. It can be seen that the impedance of the symmetrical dipole is around 50 Ω for frequencies between 1.75 and 2.4 GHz (around the 2nd and 3rd resonant frequency bands), which verifies the broadband per-

TABLE II
SIMULATED FREQUENCY BANDWIDTH OF THE BOWTIE DIPOLE

	$R = 40$ mm	$R = 50$ mm	$R = 60$ mm
$\theta = 10°$	1.93–2.14 GHz	1.83–1.93 GHz	1.58–1.97 GHz
$\theta = 30°$	1.93–2.28 GHz	1.75–2.17 GHz	1.58–1.98 GHz
$\theta = 50°$	1.91–2.25 GHz	1.73–2.19 GHz	1.55–2 GHz
$\theta = 70°$	1.91–2.28 GHz	1.73–2.21 GHz	1.55–2.03 GHz

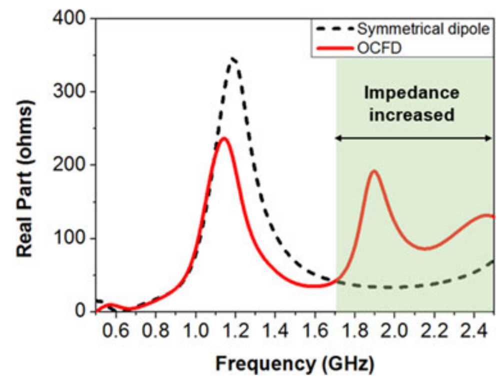

Fig. 5. Simulated real part of the impedance of the symmetrical dipole and the OCFD.

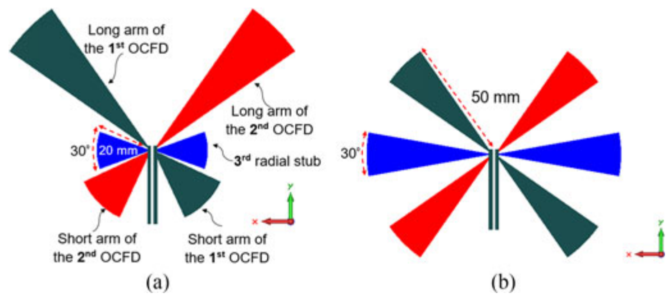

Fig. 6. (a) The proposed crossed off-center-fed dipole antenna. (b) The reference antenna with symmetrical arms for performance comparison.

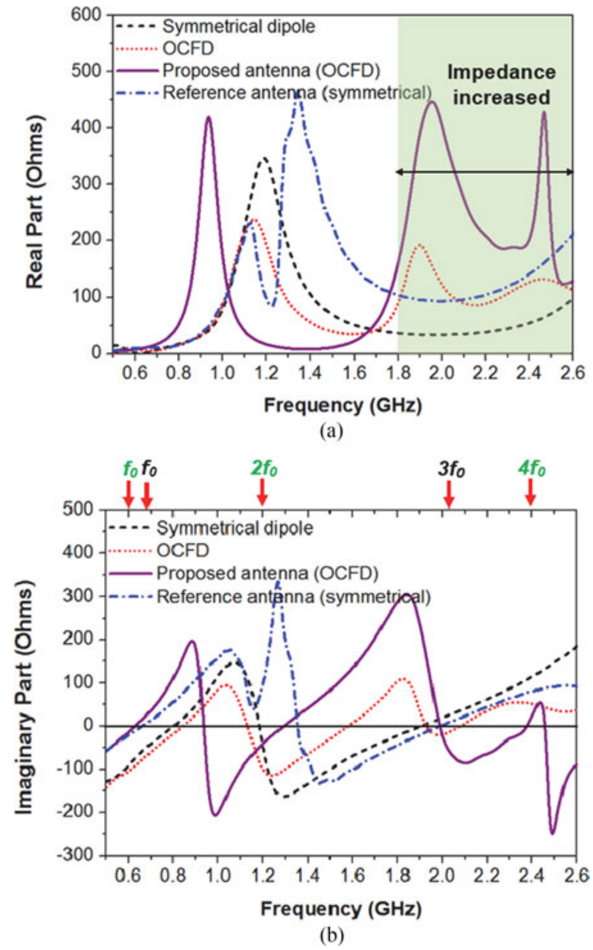

Fig. 7. Simulated input impedance of four different antennas. (a) Real part. (b) Imaginary part.

formance of the antenna as depicted in Table II. However, the impedance of the OCFD is from 100 to 200 Ω over the frequency band between 1.8 and 2.5 GHz, which is much higher than that of the symmetrical dipole. It is shown that, by modifying a broadband symmetrical bowtie dipole to an OCFD, the antenna impedance is significantly increased over the desired resonant frequency range. In addition, the impedance for both antennas at the frequencies from 1.1 to 1.2 GHz is also very high (i.e., over 200 Ω), this is due to the antiresonance of the dipole antenna [31].

The next step is to modify the proposed OCFD to a crossed OCFD by introducing another OCFD. As shown in Fig. 6(a), the second OCFD (red) has the same dimensions as the first one, but they are orthogonal to each other. The purpose is to achieve dual polarization receiving capability and generate a vertically symmetrical radiation pattern for the antenna. Finally, another pair of radial stubs (blue) is inserted between the two OCFDs to further manipulate the impedance. The final antenna layout is show in Fig. 6(a) which looks symmetrical from left to right as a whole. For comparison, a reference antenna consisting of three dipoles with symmetrical arms is studied. As shown in Fig. 6(b), the arms of the reference antenna have a radius of 50 mm and a circumference angle of 30° for the radial stub. Thus, the reference antenna and the proposed antenna have the same electrical length (100 mm). The simulated real part and imaginary part of the input impedance of four different antennas (single symmetrical dipole, single OCFD, proposed OCFD, and reference antenna) are shown in Fig. 7(a) and (b). It can be seen that the real part of the input impedance of the proposed broadband OCFD antenna is above 180 Ω (up to 450 Ω) for the frequency band between 1.8 and 2.5 GHz, which is much higher than that of the reference antenna (around 100 Ω). In addition, the proposed antenna has shifted the high-impedance (about 400 Ω) frequency from around 1.4 to around 0.9 GHz. This is likely due to the coupling effects among the three dipoles. The imaginary part of the reference antenna is around 0 Ω at frequencies around 0.7 and 2.1 GHz, which are f_0 and $3f_0$, respectively. While the imaginary part of the proposed OCFD is around 0 Ω at resonant frequencies 0.6, 1.2, and 2.4 GHz, which are f_0, $2f_0$, and $4f_0$, respectively. These results have demonstrated that the simulated results agree with the OCFD theory as discussed in Section III-A. Furthermore, the imaginary part of the impedance of the antenna over the resonant frequency band from 1.4 to 2 GHz turns from negative values (for the reference antenna) to positive values (for the proposed antenna). As shown in Fig. 7(b), the value of the imaginary part of the proposed antenna impedance varies between 0 and 300 Ω over the desired frequency band. This feature could help the proposed antenna to produce a better conjugate matching with the rectifier, since the imaginary part of the impedance of the rectifier normally varies between –700 and 0 Ω as we discussed earlier. The simulated three dimensional (3-D) radiation patterns of the proposed antenna at the frequencies of interest are depicted in Fig. 8. The two-dimensional (2-D) polar plots of antenna patterns in *E-plane* and *H-plane* are shown as well. Here, we have only showed the directivity (maximum gain) of the antenna (without taking the mismatch loss into account). From Fig. 8, it can be seen that the antenna has symmetrical patterns about YOZ plane with a maximum directivity of 1.8 dBi at 0.9 GHz, 3.5 dBi at 1.8 GHz, and 3.3 dBi at 2.4 GHz. The antenna is more directive toward the long arm direction at 1.8 and 2.4 GHz with the half-power beam-widths (HPBW) of around 174° and 185°, respectively. The HPBW is about 96° at 0.9 GHz.

Therefore, the proposed broadband OCFD antenna has obtained high impedance over a wide frequency range. The

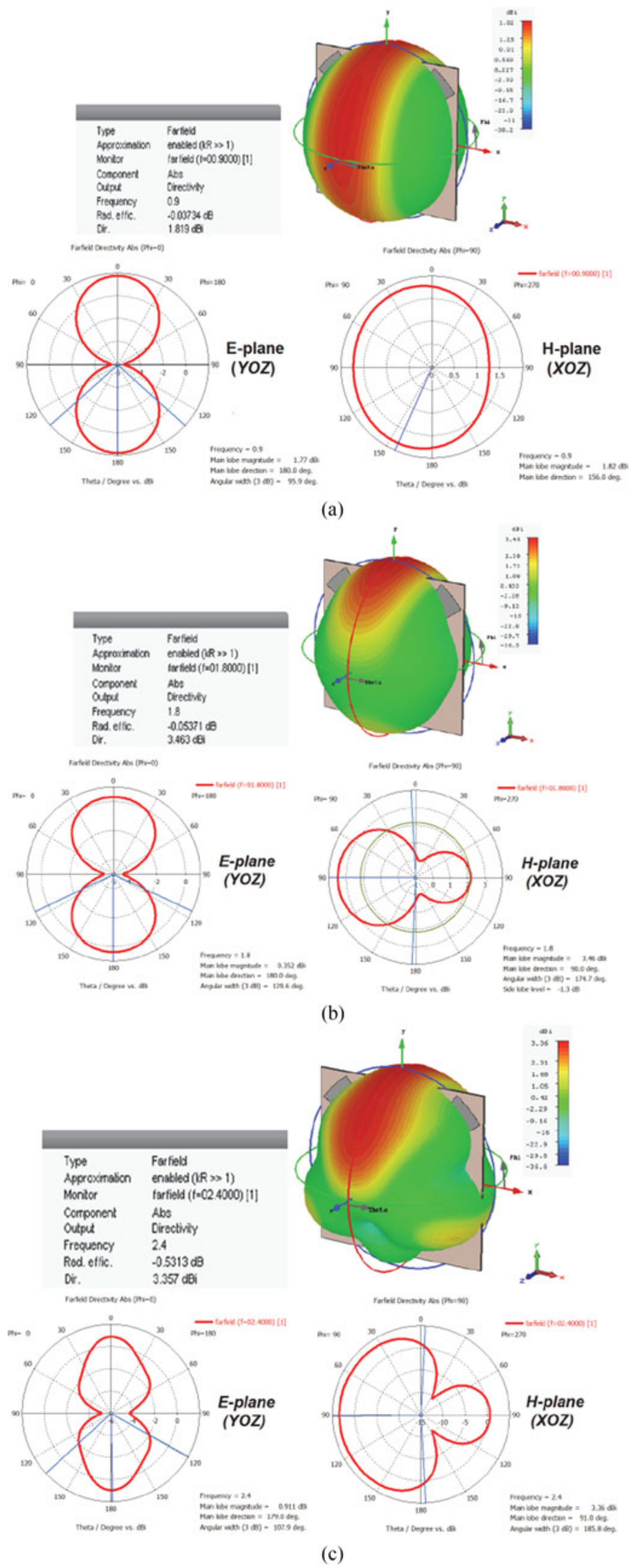

Fig. 8. Simulated 3-D patterns with directivities and 2-D patterns over *E*-plane and *H*-plane of the proposed antenna at (a) 0.9 GHz, (b) 1.8 GHz, and (c) 2.4 GHz.

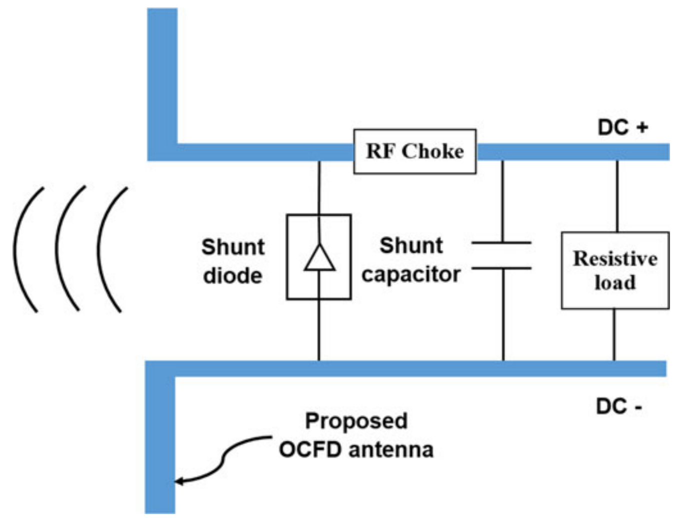

Fig. 9. Configuration of a single shunt diode (Class F) rectifier with a dipole antenna.

proposed design is just an example to illustrate the proposed new method. The details of the dipole could be modified according to the frequency of interest.

IV. Rectenna Integration

A. Rectifier Configuration

The proposed high impedance OCFD antenna may directly conjugate match with the input impedance of a rectifier over a wide frequency band. The rectifier should only consist of few circuit components for rectification, dc storage, and output. A single shunt diode rectifier is selected due to its very simple structure and high conversion efficiency [33]. The configuration of the single shunt diode rectifier with a dipole antenna is depicted in Fig. 9. The shunt diode is used as the rectifying element and the diodes for high frequency (e.g., $f > 1$ GHz) applications are normally Schottky diodes such as SMS7630 (from Skyworks) and HSMS2860 (from Avago). A shunt capacitor after the diode is used to store dc power and smooth the dc output waveforms. In addition, a series connected RF choke is placed between the diode and capacitor to block ac components generated from the diode. In this design, a typical inductor of 47 nH is selected as the RF choke. To have a better configuration on the PCB, the proposed antenna and rectifier are both fed by CPS (or twin-wire conducting strips). The topology of the rectifier configured with the conducting strips extended from the OCFD antenna is shown in Fig. 10. The values and part numbers of the circuit components are given in Table III.

The rectifier is built and simulated by using the ADS software. To improve the accuracy of results, the diode is modeled by using a nonlinear SPICE model with parasitic elements provided by the suppliers (such as Skyworks). The chip inductor and capacitor are modeled by using the real product models, including the *S*-parameter files, provided by Murata and Coilcraft. Since the proposed design can eliminate the matching network between the antenna and the rectifier, thus the rectifying circuit

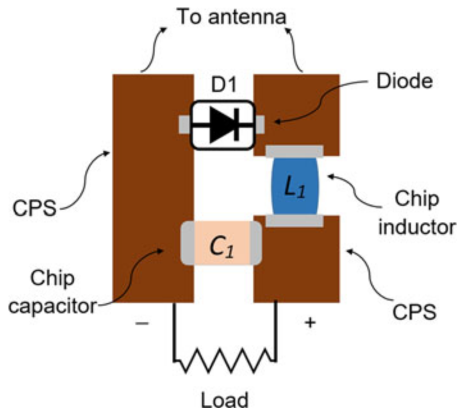

Fig. 10. Configuration of the proposed rectifier on coplanar striplines (CPS).

TABLE III
CIRCUIT COMPONENTS USED IN THE DESIGN

Component name	Nominal Value	Part number and supplier
D1	Schottky diode	SMS7630-079LF, Skyworks
L1	47 nH chip inductor	0603HP47N, Coilcraft
C1	100 nF chip capacitor	GRM188R71H104JA93D, Murata

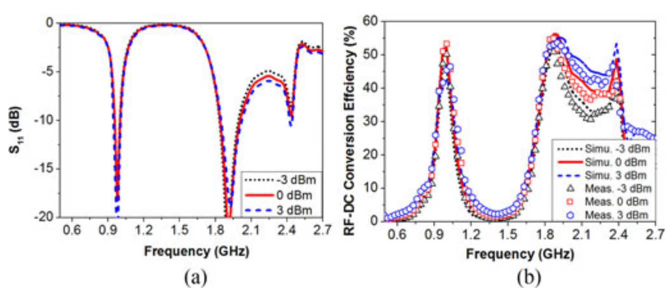

Fig. 11. (a) The simulated S_{11} and (b) the simulated and measured RF–dc conversion efficiency of the rectenna at three different input power levels. The load resistance is 400 Ω.

is indeed simplified. The frequency domain power source port is used in the simulation, and the port impedance is defined as the impedance of the proposed OCFD antenna by using the touchstone S1P files exported from the CST, similarly to the results shown in Fig. 7(a) and (b).

B. Rectenna Performance

After the complete rectenna has been designed, its performance is evaluated by using the harmonic balance simulation and the large signal *S*-parameter simulation using the ADS. The performances of the proposed rectenna in terms of the reflection coefficient (S_{11}) and RF–dc conversion efficiency are shown in Figs. 11–13. The RF–dc conversion efficiency is obtained by

$$\eta_{\mathrm{RF-dc}} = \frac{P_{\mathrm{dc}}}{P_{\mathrm{in}}} \tag{8}$$

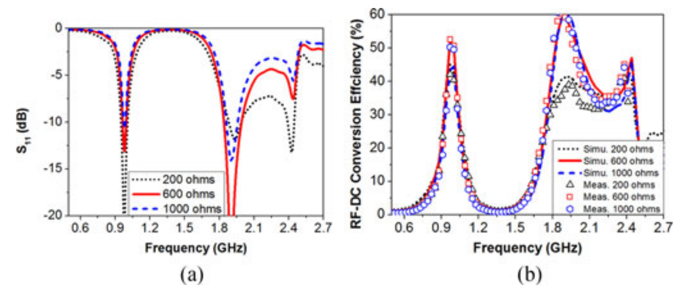

Fig. 12. (a) The simulated S_{11} and (b) the simulated and measured RF–dc conversion efficiency of the rectenna at three different load values. The input power level is 0 dBm.

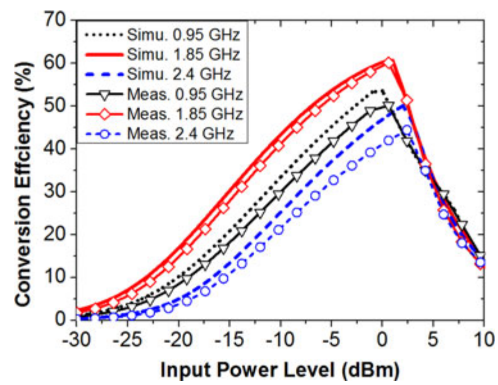

Fig. 13. Simulated and measured conversion efficiency of the rectenna versus input power level at three frequencies. The load resistance is 600 Ω.

where P_{dc} is the output dc power and *Pin* is the input RF power to the antenna. S_{11} (simulated) and conversion efficiency (simulated and measured) of the rectenna at different input power levels are shown in Fig. 11(a) and (b) as a function of frequency. A typical load resistor of 400 Ω is selected. From Fig. 11, it can be seen that the rectenna covers the desired broad frequency band from 1.8 to 2.5 GHz and an additional frequency band around 1 GHz. The S_{11} of the rectenna is lower than –10 dB between 1.8 and 2 GHz and around 1 GHz. The conversion efficiency is higher than 40% (up to 55%) over the entire frequency band of interest for the input power level of 0 dBm (1 mW). In addition, when the input power is doubled (3 dBm) or halved (–3 dBm), the reflection coefficients are always smaller than –6 dB from 1.8 to 2.5 GHz, while the efficiency over the band of interest is still high (e.g., greater than 35%).

Fig. 12(a) and (b) depicts the S_{11} (simulated) and conversion efficiency (simulated and measured) of the rectenna for different load values. It can be seen that the efficiency is higher than 30% (up to 60%) for the load values from 200 to 1000 Ω and for the frequencies between 1.8 and 2.5 and the around 1 GHz. It is demonstrated that the nonlinear effects linked to the input power and load are reduced in the proposed broadband rectenna, which verifies our predictions in Section II. The simulated and measured conversion efficiency of the rectenna versus input power level is shown in Fig. 13 at three frequencies. It can be seen that the rectenna has the highest efficiency at the input

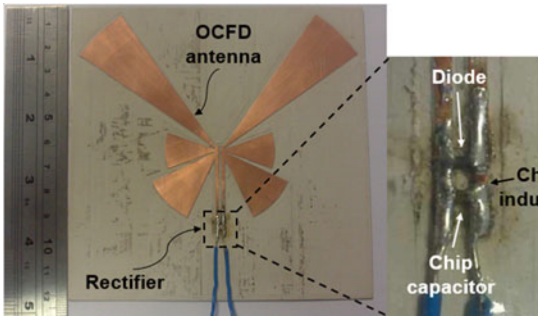

Fig. 14. Fabricated prototype rectenna. The enlarged view of the rectifier is shown as well.

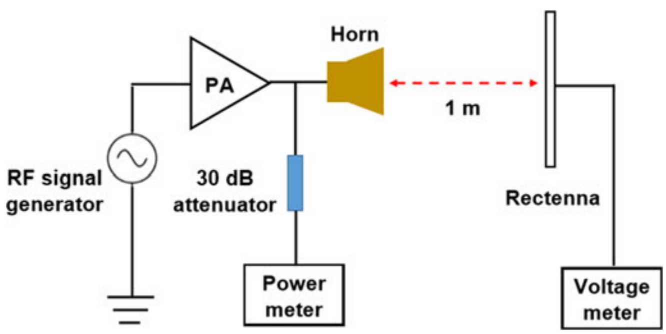

Fig. 15. Measurement setup of the rectenna.

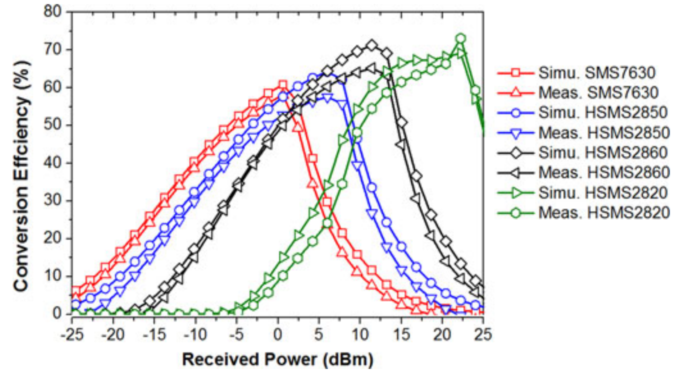

Fig. 16. Simulated and measured conversion efficiency of the rectenna versus input power level for using different types of Schottky diodes. The frequency is 1.85 GHz.

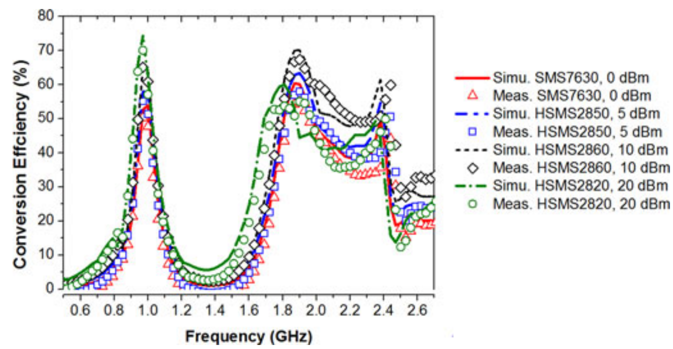

Fig. 17. Simulated and measured conversion efficiency of the rectenna versus frequency for using different types of Schottky diodes at the optimal input power levels. The load resistance is 500 Ω.

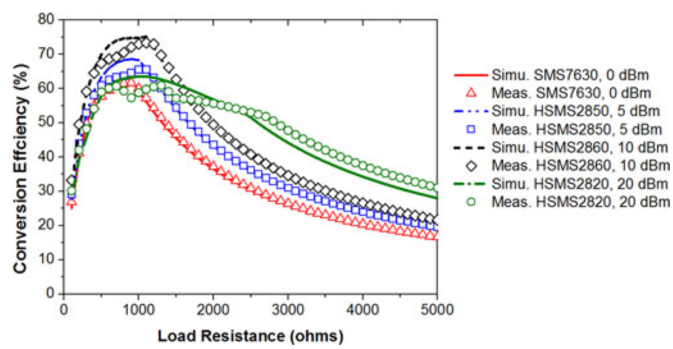

Fig. 18. Simulated and measured conversion efficiency of the rectenna versus load resistance for using different types of Schottky diodes at the optimal input power levels. The frequency is 1.85 GHz.

power of around 0 dBm. This is because the selected diode (SMS7630) has reached its reverse breakdown voltage. Since this diode has a very low forward bias voltage (150 mV) and a low breakdown voltage (2 V) [34], it is normally applied in low input power (e.g., from –30 to 0 dBm) applications. For high input power applications (e.g., >10 dBm) and higher conversion efficiency (e.g., up to 80%), other diodes with a higher breakdown voltage could be selected.

V. Rectenna Measurements and Validations

The fabricated prototype rectenna is shown in Fig. 14 and the measurement setup is depicted in Fig. 15. Since the proposed antenna has been integrated with the rectifier, S_{11} of the rectenna cannot be measured directly. A standard horn antenna R&SHF906 was used to transmit the RF power. A 30 dB gain PA amplifies the signal generated by an RF signal generator (Keithley2920). The rectenna was configured to receive the signal at a distance of 1 m (in antenna far field). The output dc voltage ($V_{\rm dc}$) was measured by using a voltage meter and the output dc power can be obtained by using $P_{\rm out} = V_{\rm dc}^2/R$, where R is the load resistance.

The available power to the transmitting horn antenna was measured by using a power meter; thus, the received RF power by the rectenna can be estimated by using the Friis transmission equation [35]

$$P_r = P_t + G_t + G_r + 20\log_{10}\frac{\lambda}{4\pi r} \quad (9)$$

where P_r is the received power in dBm, P_t is the power obtained from the power meter in dBm, Gt is the realized gain of the transmitting antenna in dB, Gr is the realized gain of the receiving antenna (rectenna) in dB, λ is the wavelength, and r is the distance between the TX and RX antennas ($r = 1$ m).

As discussed earlier, the proposed rectenna can reduce the effects of the nonlinearity of the rectifier and match well to a wide range of load impedance values. Thus, the rectenna may perform well even when different types of diodes are used.

TABLE IV
RECTENNA PERFORMANCE FOR USING DIFFERENT DIODES

Schottky diodes name	Simulated input impedance under the same condition (Ω)	Optimal input power level	Maximum conversion efficiency	Optimal load resistance range (Ω)
SMS7630	173 – *j* 36	0 dBm	60%	250–1500
HSMS2850	325 – *j* 57	5 dBm	65%	200–2000
HSMS2860	349 – *j* 166	10 dBm	70%	200–2500
HSMS2820	82 – *j* 145	20 dBm	75%	250–3000

This advantage is normally not available in the conventional rectenna designs, since the input impedance and characteristics of the diodes can be very different. Thus, in order to validate this point, the proposed rectenna was measured by using different types of Schottky diodes such as HSMS2850, HSMS2860, and HSMS2820. The measured conversion efficiency versus input power level is shown in Fig. 16 along with simulated results. High conversion efficiency is obtained in all cases. When the load is selected as 500 Ω and the frequency is selected as 1.85 GHz, we have $Gt = 8.5\,\text{dBi}$, $Gr = 3.45\,\text{dBi}$, $\lambda = 0.162\,\text{m}$, and $r = 1\,\text{m}$. Using (9), the correlation between the transmitting power and the receiving power can be obtained as

$$\text{Pr}\,(\text{dBm}) = \text{Pt}\,(\text{dBm}) - 25.84\text{ dB}. \tag{10}$$

It can be seen that the maximum conversion efficiency and the corresponding input powers of the rectenna are 60% at 0 dBm, 65% at 5 dBm, 70% at 10 dBm, and 75% at 20 dBm for using the Schottky diodes SMS7630, HSMS2850, HSMS2860, and HSMS2820, respectively. The peak efficiency is realized at different input power levels. This is because the breakdown voltages for the selected diodes are different, which are 2 V (SMS7630), 3.8 V (HSMS2850), 7 V (HSMS2860), and 15 V (HSMS2820), respectively. The efficiency is much higher at high input power levels for using the diodes with large breakdown voltages (e.g., HSMS2820), while the efficiency is higher at low input power levels for using the diodes with small forward bias voltages (e.g., SMS7630). The simulated and measured conversion efficiencies of the rectenna (using the four different diodes) are depicted in Fig. 17 as a function of the frequency. The load is still 500 Ω while the input power levels are selected as the optimal input powers for these diodes (e.g., 0 dBm for SMS7630, 5 dBm for HSMS2850, 10 dBm for HSMS2860, and 20 dBm for HSMS2820). Note that in the measurements, the correlation between the transmitting power and the receiving power [as given in (9)] might be changed if the frequencies are different. Thus, the transmitting power should be tuned to make sure that the received power is approximately a constant value in the broadband (e.g., 0 dBm for the frequencies from 0.9 to 3 GHz).

From the results in Fig. 17, it can be seen that the rectenna is still of broadband performance (1.8 to 2.5 GHz) when using different diodes, and the conversion efficiency is constantly high over the frequency bandwidth of interest for the selected input power levels. Figs. 16 and 17 show a good agreement between the simulated and measured results.

Fig. 18 shows the simulated and measured conversion efficiency by using different load resistances. The frequency is selected as 1.85 GHz while the input power levels are still set as the optimal input powers. In reality, the load impedance may vary over a large range in different applications; thus, it is important to reduce the sensitivity of efficiency versus load variation in a nonlinear system (rectenna). From Fig. 18, it can be seen that, when using different diodes, the efficiency of the rectenna is constantly high (from 40% to 75%) for the load values between 200 and 2000 Ω, then the efficiency starts to decease due to the impedance mismatch between the antenna and the rectifier. It demonstrates that the nonlinear effects have been reduced over the load range from 200 to 2000 Ω. For other load values, the details of the rectenna can be modified to achieve good performance.

According to the results in Figs. 16–18, the performance of the rectenna by using different diodes is summarized in Table IV. The simulated input impedance of the rectifier is shown under the same condition (frequency: 1.85 GHz, input power: 10 dBm, and load: 500 Ω). The impedance is very different for different types of diodes, but our rectenna can still be well configured with these diodes without using matching networks. It is demonstrated that the proposed broadband rectenna can work well under different operating conditions. The nonlinear effects have been reduced. The matching networks have indeed been eliminated. In addition, the optimal input power level of the device is tunable (from 0 to 23 dBm) by selecting appropriate diodes so that the conversion efficiency of the broadband rectenna can be always higher than 60% (as shown in Fig. 16). This is very important for WPT or WEH used in practice.

A comparison between our rectennna and other related work is shown in Table V. It can be seen that our design seems to be the only one without using the matching networks, but still achieves high conversion efficiency over a relatively wide frequency band. The conversion efficiency of our design is comparable with that of the other work used matching networks, while the performance of the rectenna is reasonably well in a range of input powers and load impedance. In addition, our device is also the only one which can use different types of diodes without changing any other part of the circuit. The structure of our design is the simplest for broadband rectennas with similar performance. The proposed rectenna is of good industrial value due to its simplicity and universality, and is of good practical value due to its consistent performance under different operating conditions.

Also, the proposed concept for eliminating the matching networks is not just limited in the presented design, and can also be used in other similar nonlinear systems.

TABLE V
COMPARISON OF THE PROPOSED RECTENNA AND RELATED DESIGNS

Ref. (year)	Frequency (GHz)	Use of impedance matching networks	Complexity of the overall design	Maximum conversion efficiency (%)	Input power level for conversion efficiency > 60%	Optimal load range with good performance (kΩ)	Type of Schottky diode
[18] (2015)	Four-band 0.9, 1.8, 2.1, 2.4	Yes	Very complex	65 at 0 dBm	–5 to 0 dBm	11	MSS20-141
[19] (2015)	Broad-band 1.8–2.5	Yes	Complex	70 at 0 dBm	–7 to 0 dBm	14.7	SMS7630
[20] (2015)	Dual-band 0.915, 2.45	Yes	Complex	70 at 0 dBm	–5 to 0 dBm	0.5–3	SMS7630
[23] (2012)	Tunable 0.9–2.45	Yes	Very complex	80 at 30 dBm	Tunable 5 to 30 dBm	1–4	Tunable
[24] (2016)	Six-band 0.55, 0.75, 0.9, 1.85, 2.15, 2.45	Yes	Very complex	68 at –5 dBm	–5 to 0 dBm	10–75	SMS7630
[25] (2012)	Single-band 2.45	No	Simple	70 at –5 dBm	–10 to 5 dBm	2.8	HSMS2852
[26] (2004)	Broad-band 2–18	No	Medium	20 at 17 dBm	Not available	0.6	SMS7630
This work (2016)	**Broad-band 0.9–1.1, 1.8–2.5**	**No**	**Simplest**	**75 at 20 dBm**	**Tunable 0 to 23 dBm**	0.2–2	**Tunable**

VI. CONCLUSION

A novel method for eliminating the matching network of broadband rectennas was presented. An OCFD antenna was designed, where the antenna impedance was tuned to directly match with the rectifier. The proposed rectenna was of a broad bandwidth and high efficiency, and had excellent performance under different operating conditions. The measured performance showed that the operating frequencies of the experimental rectenna were from 0.9 to 1.1 GHz and from 1.8 to 2.5 GHz (which were the typical cellular mobile, WLAN, and ISM bands), while the maximum conversion efficiency was up to 75% and the optimal input power range was tunable from 0 to 23 dBm by selecting appropriate diodes. In addition, the rectenna had a very simple structure and low cost. Considering the excellent overall performance of the proposed rectenna, it is suitable for high efficiency WPT and WEH applications. The design concept is easy to follow while its details can be optimized for different applications.

ACKNOWLEDGMENT

The authors would like to thank the anonymous reviewers for their constructive feedback of this paper. The authors would also like to thank Prof. S. Hall from the University of Liverpool for the refinement of the manuscript.

REFERENCES

[1] S. Carreon-Bautista, A. Eladawy, A. N. Mohieldin, and E. Sanchez-Sinencio, "Boost converter with dynamic input impedance matching for energy harvesting with multi-array thermoelectric generators," *IEEE Trans. Ind. Electron.*, vol. 61, no. 10, pp. 5345–5353, Oct. 2014.

[2] J. Jeong and D. Jang, "Design technique for harmonic-tuned RF power oscillators for high-efficiency operation," *IEEE Trans. Ind. Electron.*, vol. 62, no. 1, pp. 221–228, Jan. 2015.

[3] J. Kim, D.-H. Kim, and Y.-J. Park, "Analysis of capacitive impedance matching networks for simultaneous wireless power transfer to multiple devices," *IEEE Trans. Ind. Electron.*, vol. 62, no. 5, pp. 2807–2813, May 2015.

[4] K. Song and Q. Xue, "Ultra-wideband ring-cavity multiple-way parallel power divider," *IEEE Trans. Ind. Electron.*, vol. 60, no. 10, pp. 4737–4745, Oct. 2013

[5] K. Rawat and F. M. Ghannouchi, "Design methodology for dual-band Doherty power amplifier with performance enhancement using dualband offset lines," *IEEE Trans. Ind. Electron.*, vol. 59, no. 12, pp. 4831–4842, Dec. 2012

[6] X. Wang, X. K. Guan, and S. Q. Fan, "ESD-protected power amplifier design in CMOS for highly reliable RFICs," *IEEE Trans. Ind. Electron.*, vol. 58, no. 7, pp. 2736–2743, Jun. 2011.

[7] R. Johari, J. V. Krogmeier, and D. J. Love, "Analysis and practical considerations in implementing multiple transmitters for wireless power transfer via coupled magnetic resonance," *IEEE Trans. Ind. Electron.*, vol. 61, no. 4, pp. 1174–1183, Apr. 2014.

[8] L. Chen, Y. C. Zhou, and T. J. Cui, "An optimizable circuit structure for high-efficiency wireless power transfer," *IEEE Trans. Ind. Electron.*, vol. 60, no. 1, pp. 339–349, Jan. 2013.

[9] H. J. Visser and R. J. M. Vullers, "RF energy harvesting and transport for wireless sensor network applications: Principles and requirements," *Proc. IEEE*, vol. 101, no. 6, pp. 1410–1423, Jun. 2013.

[10] S. Cheon, Y.-H. Kim, S.-Y. Kang, M. L. Lee, J.-M. Lee, and T. Zyung, "Circuit-model-based analysis of a wireless energy-transfer system via coupled magnetic resonances," *IEEE Trans. Ind. Electron.*, vol. 58, no. 7, pp. 2906–2914, Jul. 2011.

[11] J. Colomer-Farrarons, P. Miribel-Català, A. Saiz-Vela, and J. Samitier, "A multiharvested self-powered system in a low-voltage low-power technology," *IEEE Trans. Ind. Electron.*, vol. 58, no. 9, pp. 4250–4263, Sep. 2011.

[12] Y. Huang, N. Shinohara, and T. Mitani, "A constant efficiency of rectifying circuit in an extremely wide load range," *IEEE Trans. Microw. Theory Techn.*, vol. 62, no. 4, pp. 986–993, Apr. 2014.

[13] P. Lu, X. Yang, J. Li, and B. Wang, "A compact frequency reconfigurable rectenna for 5.2- and 5.8-GHz wireless power transmission," *IEEE Trans. Power Electron.*, vol. 30, no. 11, pp. 6006–6010, Nov. 2015.

[14] J. O. McSpadden, F. Lu, and K. Chang, "Design and experiments of a high conversion efficiency 5.8-GHz rectenna," *IEEE Trans. Microw. Theory Techn.*, vol. 46, no. 12, pp. 2053–2060, Dec. 1998.

[15] H. Sun, Y.-X. Guo, M. He, and Z. Zhong, "A dual-band rectenna using broadband Yagi antenna array for ambient RF power harvesting," *IEEE Antennas Wireless Propag. Lett.*, vol. 12, pp. 918–921, 2013.

[16] K. Niotaki, S. Kim, S. Jeong, A. Collado, A. Georgiadis, and M. Tentzeris, "A compact dual-band rectenna using slot-loaded dual band folded dipole antenna," *IEEE Antennas Wireless Propag. Lett.*, vol. 12, pp. 1634–1637, 2013.

[17] R. Scheeler, S. Korhummel, and Z. Popovic, "A dual-frequency ultralow-power efficient 0.5-g rectenna," *IEEE Microw. Mag.*, vol. 15, no. 1, pp. 109–114, Jan. 2014.

[18] V. Kuhn, C. Lahuec, F. Seguin, and C. Person, "A multi-band stacked RF energy harvester with rf-to-dc efficiency up to 84%," *IEEE Trans. Microw. Theory Techn.*, vol. 63, no. 5, pp. 1768–1778, May 2015.

[19] C. Song, Y. Huang, J. Zhou, J. Zhang, S. Yuan, and P. Carter, "A high-efficiency broadband rectenna for ambient wireless energy harvesting," *IEEE Trans. Antennas Propag.*, vol. 63, no. 8, pp. 3486–3495, May 2015.

[20] K. Niotaki, A. Georgiadis, A. Collado, and J. S. Vardakas, "Dual-band resistance compression networks for improved rectifier performance," *IEEE Trans. Microw. Theory Techn.*, vol. 62, no. 12, pp. 3512–3521, Nov. 2015.

[21] Y. Han, O. Leitermann, D. A. Jackson, J. M. Rivas, and D. J. Perreault, "Resistance compression networks for radio-frequency power conversion," *IEEE Trans. Power Electron.*, vol. 22, no. 1, pp. 41–53, Jan. 2007.

[22] T. Paing, J. Shin, R. Zane, and Z. Popovic, "Resistor emulation approach to low-power RF energy harvesting," *IEEE Trans. Power Electron.*, vol. 23, no. 3, pp. 1494–1501, Mar. 2008.

[23] V. Marian, B. Allard, C. Vollaire, and J. Verdier, "Strategy for microwave energy harvesting from ambient field or a feeding source," *IEEE Trans. Power Electron.*, vol. 27, no. 11, pp. 4481–4491, Nov. 2012.

[24] C. Song *et al.*, "A novel six-band dual CP rectenna using improved impedance matching technique for ambient RF energy harvesting," *IEEE Trans. Antennas Propag.*, vol. 64, no. 7, pp. 3160–3171, Jul. 2016.

[25] H. Sun, Y.-X. Guo, M. He, and Z. Zhong, "Design of a high-efficiency 2.45-GHz rectenna for low-input-power energy harvesting," *IEEE Antennas Wireless Propag. Lett.*, vol. 11, pp. 929–932, 2012.

[26] J. A. Hagerty, F. B. Helmbrecht, W. H. McCalpin, R. Zane, and Z. B. Popovic, "Recycling ambient microwave energy with broad-band rectenna arrays," *IEEE Trans. Microw. Theory Techn.*, vol. 52, no. 3, pp. 1014–1024, Mar. 2004.

[27] Z. K. Ma and G. A. E. Vandenbosch, "Wideband harmonic rejection filtenna for wireless power transfer," *IEEE Trans. Antennas Propag.*, vol. 62, no. 1, pp. 371–377, Oct. 2013.

[28] N. Shinohara and Y. Zhou, "Development of rectenna with high impedance and high Q antenna," in *Proc. 2014 Asia–Pac. Microw. Conf.*, Nov. 2014, pp. 600–602.

[29] H. Miyagoshi, K. Noguchi, K. Itoh, and J. Ida, "High-impedance wideband folded dipole antenna for energy harvesting applications," in *Proc. 2014 Int. Symp. Antennas Propag.*, Dec. 2014, pp. 601–602.

[30] H. Chu, Y.-X. Guo, and Z. Wang, "60-GHz LTCC wideband vertical offcenter dipole antenna and arrays," *IEEE Trans. Antennas Propag.*, vol. 61, no. 1, pp. 153–161, Jan. 2013.

[31] R. Li, L. Pan, and Y. Cui, "A novel broadband circularly polarized antenna based on off-center-fed dipoles," *IEEE Trans. Antennas Propag.*, vol. 63, no. 12, pp. 5296–5304, Dec. 2015.

[32] J. Belrose and P. Bouliane, "The off-center-fed dipole revisited: a broadband, multiband antenna," *QST Mag.*, vol. 74, no. 8, pp. 28–34, 1990.

[33] J. Guo, H. Zhang, and X. Zhu, "Theoretical analysis of RF–DC conversion efficiency for class-F rectifiers," *IEEE Trans. Microw. Theory Techn.*, vol. 62, no. 4, pp. 977–985, Apr. 2014.

[34] *Surface Mount Mixer and Detector Schottky Diodes*, *Data Sheet.* Skyworks Solutions, Inc., Woburn, MA, USA, 2013.

[35] S. Ladan, A. B. Guntupalli, and K. Wu, "A high-efficiency 24 GHz rectenna development towards millimeter-wave energy harvesting and wireless power transmission," *IEEE Trans. Circuits Syst. I, Reg. Papers*, vol. 61, no. 12, pp. 3358–3366, Dec. 2014.

[36] J. D. Kraus and R. J. Marhefka, *Antennas: For All Applications*, 3rd ed. New York, NY, USA: McGraw-Hill, 2001.

[37] S. Schellkunoff, *Electromagnetic Waves*. New York, NY, USA: Van Nostrand, 1943.

[38] E. Spingola, "Multiband HF antennas, part 3, Windom and OCF dipole," *Communicator*, vol. 13, no. 4, pp. 7–11, 2010.

Chaoyun Song (S'16) received the B.Eng. (Hons.) degree in telecommunication engineering from Xi'an Jiaotong-Liverpool University, Suzhou, China, in 2012, and the M.Sc. degree with distinction in microelectronics and telecommunication in 2013 from the University of Liverpool, Liverpool, U.K., where he is currently working toward the Ph.D. degree in wireless communications and radio frequency engineering.

His current research interests include rectifying antennas, circular polarization antennas, power management circuits, wireless power transfer and energy harvesting, and wearable antennas.

Mr. Song has been a Regular Reviewer for the IEEE TRANSACTIONS ON CIRCUITS AND SYSTEMS I: REGULAR PAPERS, IEEE TRANSACTIONS ON MICROWAVE THEORY AND TECHINQUES, and IEEE ANTENNAS AND WIRELESS PROPAGATION LETTERS.

Yi Huang (S'91–M'96–SM'06) received the D.Phil. degree in communications from the University of Oxford, Oxford, U.K., in 1994.

In 1995, he oined the Department of Electrical Engineering and Electronics, University of Liverpool, Liverpool, U.K., where he is currently a Full Professor in wireless engineering. He has published more than 200 refereed papers in leading international journals and conference proceedings, and is the principal author of the popular book *Antennas: From Theory to Practice* (Wiley, 2008). He has been conducting research in the areas of wireless communications, applied electromagnetics, radar, and antennas for the past 25 years.

Prof. Huang has been an Editor, an Associate Editor, or a Guest Editor of four international journals. He is at present the Editor-in-Chief of *Wireless Engineering and Technology*, an Associate Editor of the IEEE ANTENNAS AND WIRELESS PROPAGATION LETTERS, a U.K. National Representative of the European COST-IC1102, a Fellow of the Institution of Engineering and Technology (IET), U.K., and an Executive Committee Member of the IET Electromagnetics PN.

Jiafeng Zhou received the B.Sc. degree in radio physics from Nanjing University, Nanjing, China, in 1997, and the Ph.D. degree from the University of Birmingham, Birmingham, U.K., in 2004. His Ph.D. research concerned high-temperature superconductor microwave filters.

Beginning in 1997, for two and a half years, he was with the National Meteorological Satellite Centre of China, Beijing, China, where he was involved in the development of communication systems for Chinese geostationary meteorological satellites. From 2004 to 2006, he was a Research Fellow with the University of Birmingham, where he was involved in phased arrays for reflector observing systems. Until 2013, he was with the Department of Electronic and Electrical Engineering, University of Bristol, Bristol, U.K., where he was involved in the development of highly efficient and linear amplifiers. He is currently with the Department of Electrical Engineering and Electronics, University of Liverpool, Liverpool, U.K. His current research interests include microwave power amplifiers, filters, electromagnetic energy harvesting, and wireless power transfer.

Paul Carter received the B.Sc. degree (Hons.) in physics from the University of Manchester, Manchester, U.K., in 1987, and the M.Sc. degree (Eng.) in microelectronic systems and telecommunications and the Ph.D. degree in electrical engineering and electronics from the University of Liverpool, Liverpool, U.K., in 1988 and 1991, respectively.

He is the President and the CEO of Global Wireless Solutions, Inc. (GWS), Dulles, VA, USA, a leading independent benchmarking solution vendor for the wireless industry. With more than 25 years of experience in the cellular network industry, he founded GWS to provide operators with access to in-depth, accurate network benchmarking, analysis, and testing. Prior to GWS, he directed business development and CDMA engineering efforts for LLC, the world's largest independent wireless engineering company.

Sheng Yuan received the B.Eng. degree (first class) in microelectronics and telecommunication engineering and the Ph.D. degree in electrical engineering and electronics from the University of Liverpool, Liverpool, U.K., in 2012 and 2016, respectively.

He is currently with the Department of Intelligent Transportation Systems, Arup Group Limited, Newcastle, U.K. His research interests include wireless energy harvesting, ferromagnetic materials, indoor navigation systems, energy management circuits, wireless power transfer, radio-frequency identification, and intelligent transportation systems.

Qian Xu received the B.Eng. and M.Eng. degrees in electrical engineering and electronics from the Department of Electronics and Information, Northwestern Polytechnical University, Xi’an, China, in 2007 and 2010, respectively, and the Ph.D. degree in electrical engineering from the University of Liverpool, Liverpool, U.K., in 2016.

He is currently an Associate Professor in the College of Electronic and Information Engineering, Nanjing University of Aeronautics and Astronautics, Nanjing, China. He worked as an RF Engineer in Nanjing, China, in 2011, an Application Engineer at CST Company, Shanghai, China, in 2012, and a Research Assistant at the University of Liverpool in 2016. His research interests include statistical electromagnetics, reverberation chambers, computational electromagnetics, and anechoic chambers.

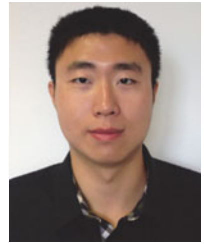

Zhouxiang Fei was born in Xi’an, China, in 1990. He received the B.Eng. degree in electronics and information engineering from Northwestern Polytechnical University, Xi’an, China, in 2012, and the M.Sc. degree with distinction in wireless communications from the University of Southampton, Southampton, U.K., in 2013. He is currently working toward the Ph.D. degree at the University of Liverpool, Liverpool, U.K.

His research interests include numerical and experimental studies of crosstalk in complex cable bundles, with a particular emphasis on considering parameter variability using efficient statistical approaches.

Mr. Fei received a student scholarship from the IEEE Electromagnetic Compatibility Society to attend the 2016 IEEE International Symposium on EMC, held in Ottawa, ON, Canada. He was also selected as a Best EMC Paper Finalist at the 2016 IEEE International Symposium on EMC.

Matching Network Elimination in Broadband Rectennas for High-Efficiency Wireless Power Transfer and Energy Harvesting

Chaoyun Song, Yi Huang, *Senior Member, IEEE*, Jiafeng Zhou, Paul Carter, Sheng Yuan, Qian Xu, and Zhouxiang Fei

***Abstract*—Impedance matching networks for nonlinear devices such as amplifiers and rectifiers are normally very challenging to design, particularly for broadband and multiband devices. A novel design concept for a broadband high-efficiency rectenna without using matching networks is presented in this paper for the first time. An off-center-fed dipole antenna with relatively high input impedance over a wide frequency band is proposed. The antenna impedance can be tuned to the desired value and directly provides a complex conjugate match to the impedance of a rectifier. The received RF power by the antenna can be delivered to the rectifier efficiently without using impedance matching networks; thus, the proposed rectenna is of a simple structure, low cost, and compact size. In addition, the rectenna can work well under different operating conditions and using different types of rectifying diodes. A rectenna has been designed and made based on this concept. The measured results show that the rectenna is of high power conversion efficiency (more than 60%) in two wide bands, which are 0.9–1.1 and 1.8–2.5 GHz, for mobile, Wi-Fi, and ISM bands. Moreover, by using different diodes, the rectenna can maintain its wide bandwidth and high efficiency over a wide range of input power levels (from 0 to 23 dBm) and load values (from 200 to 2000 Ω). It is, therefore, suitable for high-efficiency wireless power transfer or energy harvesting applications. The proposed rectenna is general and simple in structure without the need for a matching network hence is of great significance for many applications.**

***Index Terms*—Broadband rectennas, impedance matching networks, off-center-fed dipole (OCFD), wireless energy harvesting (WEH), wireless power transmission.**

Manuscript received July 5, 2016; revised October 17, 2016 and November 14, 2016; accepted December 3, 2016. This work was supported in part by the Engineering and Physical Sciences Research Council, U.K., and in part by Aeternum LLC. *(Corresponding Author: Yi Huang.)*

C. Song, Y. Huang, J. Zhou, S. Yuan, and Z. Fei are with the Department of Electrical Engineering and Electronics, University of Liverpool, Liverpool, L69 3GJ, U.K. (e-mail: sgcsong2@liv.ac.uk; Yi.Huang@liv.ac.uk; zhouj@liverpool.ac.uk; sgsyuan@liverpool.ac.uk; zf1g12@liverpool.ac.uk).

P. Carter is with Global Wireless Solutions, Inc., Dulles, VA 20166 USA (e-mail: pcarter@gwsolutions.com).

Q. Xu is with the College of Electronic and Information Engineering, Nanjing University of Aeronautics and Astronautics, Nanjing 211106, China (e-mail: emxu@foxmail.com).

Color versions of one or more of the figures in this paper are available online at http://ieeexplore.ieee.org

Digital Object Identifier 10.1109/TIE.2016.2645505

I. Introduction

IMPEDANCE matching is a basic but crucial concept in electronics and electrical engineering, since it can maximize the power transfer from a source to a load or minimize the signal reflection from a load. In the wireless industry today, there have been many devices (such as oscillators, inverters, amplifiers, rectifiers, power dividers, boost converters) and systems that have a high demand for impedance matching networks. A number of techniques for the network design have been reported [1]–[6]. Among them, rectifiers and power amplifiers (PAs) normally utilize nonlinear elements such as diodes and transistors in the circuits. Hence their input impedance varies with the frequency, input power, and load impedance. The impedance matching networks for such nonlinear circuits become very challenging to design.

Wireless power transfer (WPT) and wireless energy harvesting (WEH) have attracted significant attention in the past few years [7]–[10]. In both radiative and inductive wireless power transmissions, the rectifiers are a vital device for converting ac or RF power to dc power, while impedance matching networks are required to achieve high conversion efficiency [9].

A rectifying antenna (*rectenna*) is one of the most popular devices for WPT and WEH applications, and much progress has been made [11]–[19]. Multiband and broadband rectennas [15]–[19] can receive or harvest RF power from different sources and from different channels simultaneously; thus, they outperform the conventional single band rectennas [11]–[14] in terms of overall conversion efficiency as well as total output power. However, the design of the impedance matching network for broadband or multiband rectennas is very challenging, and the structure of the matching network is relatively complex which may increase the cost and loss, and also introduce errors in manufacturing.

Some techniques such as resistance compression networks and frequency selective networks have been developed to reduce the nonlinear effects of the rectenna [20]–[24] so that the performance can be maintained under different operating conditions. But, they all require introduction of further circuit components in the matching network which increases the complexity of the overall design. Using more components could increase the loss and decrease the overall efficiency. A need exists, therefore, for rectennas comprising simple structures

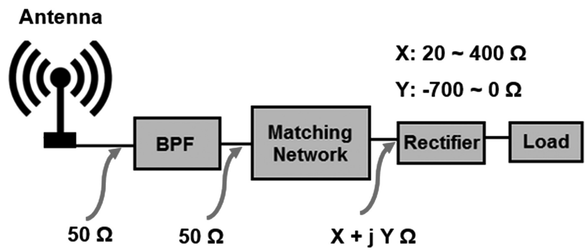

Fig. 1. Configuration of a conventional rectifying antenna system with impedance matching networks.

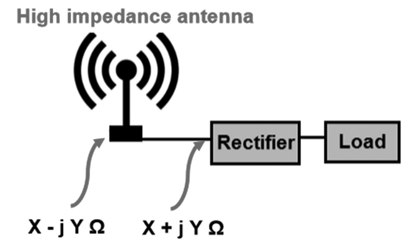

Fig. 2. Configuration of the proposed rectifying antenna without using impedance matching networks.

with competitive performance. It is desirable that the impedance matching network is eliminated or simplified, but the received RF power at different frequency bands can still be delivered to the rectifier with high RF–dc conversion efficiency.

Some designs use a standard antenna with 50 Ω impedance to match with a rectifier. Thus, either the operating bandwidth is narrow [25], or the conversion efficiency over the broadband is low, typically $<20\%$ [26]. So far there are no available designs without matching networks, that can produce high conversion efficiency over a wide frequency band, and there are no available approaches that can tune the antenna impedance to the desired value to match with the impedance of the rectifier.

In this paper, we propose a novel methodology for a high-efficiency broadband rectenna without the use of a matching network. The concept and operating mechanism are introduced in Section II. The approaches for designing a broadband high impedance antenna are discussed in Section III. The rectenna integration that can eliminate the use of matching networks is shown in Section IV. The experimental validations and measurements of a fabricated rectenna example are shown in Section V. To the best of our knowledge, the proposed design is the first broadband rectenna without using matching networks and achieves good performance; that is, high RF–dc conversion efficiency and improved linearity over a wide frequency band, a range of input power levels, and load impedance.

II. Novelty of This Work

A conventional rectifying antenna system, as shown in Fig. 1, normally consists of five different parts.

1) First of all, a receiving antenna is normally configured to receive signals from a predetermined source (WPT) or to receive random signals in the ambient environment (WEH). The input impedance of the antenna is usually matched to standard 50 Ω.
2) Secondly, a band pass filter is required to reject the higher order harmonic signals generated by the rectifier, since the signals could be radiated by the antenna which might reduce the overall conversion efficiency and cause interference. In some cases, the filter can either be embedded with the antenna to produce a filtering-antenna structure [27] or be integrated with the impedance matching network [18] to make the complete design simple and compact.
3) Thirdly, in order to match the complex impedance of the rectifier to a resistive port (e.g., 50 Ω), an impedance matching network is usually placed between the antenna and the rectifier. Thus, the power of the received signals could be fully delivered to the rectifier.
4) Fourthly, for rectification, a rectifier is configured to convert RF power to dc power. The input impedance of the rectifier varies in a wide range of values and the impedance is very sensitive to the variation of frequency, input power, and load impedance.
5) Finally, a resistive load is necessary for applications. The load could typically be a resistor, a dc-to-dc boost converter for realizing a higher output voltage, or a super capacitor to store energy.

In previous studies [18], [24], the impedance of the rectifier was analyzed under different operating conditions such as a wide frequency range (e.g., 0.5–3 GHz), a range of input powers (e.g., –40 to 0 dBm), and a wide load impedance range (e.g., 1–100 kΩ). It is concluded that the input impedance of the rectifier varies significantly (20–400 Ω for the real part, 0 to –700 Ω for the imaginary part) over these operating conditions. Furthermore, due to nonlinearity, the impedance of the rectifier would also vary with different types of rectifying diodes and different circuit topologies. However, as shown in Fig. 1, most parts are connected by using a 50 Ω port in the conventional rectenna configuration. Therefore, the design of the impedance matching network is usually the most challenging part, particularly in multiband or broadband rectennas. Thus, in previous work [19], [24], the structures of the impedance matching networks were complex for broadband and multiband rectennas, while the number of circuit components used in the matching network was very large (i.e., more than 25 elements) to reduce the nonlinear effects and produce a consistent performance. Consequently, the complex matching networks may introduce errors from manufacture, increase the cost and loss, and create additional problems.

In this work, we propose a novel method for broadband or multiband rectenna designs. The aim is to eliminate the need for impedance matching networks and to improve the overall performance of the rectenna. As shown in Fig. 2, the proposed new configuration only consists of three parts, wherein the antenna is changed to a special high impedance antenna which is very different from conventional ones. The impedance of the antenna is around 200–300 Ω for the real part and 0–300 Ω for the imaginary part in desired frequency band. The value of the antenna impedance ($X - jY$) may directly conjugate match with the input impedance of a specific rectifier ($X + jY$) within the desired frequency range but mismatch at other frequencies

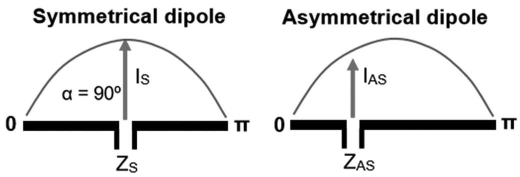

Fig. 3. Half-wavelength center-fed symmetrical dipole and the off-center-fed asymmetrical dipole.

TABLE I
SIMULATED INPUT IMPEDANCE OF THE OFF-CENTER-FED DIPOLE

Long arm (mm)	Short arm (mm)	Real part at f_0 (Ω)	Imaginary part at f_0 (Ω)
90	10	320	–213
80	20	165	–30
70	30	102	–0.8
60	40	79	5.6
50	50	73	6.4

(to produce a filtering response), as depicted in Fig. 2. Thus, a matching network can be eliminated and the proposed rectenna can offer high conversion efficiency over a broad bandwidth. Moreover, since both the rectifier and the antenna are of relatively high input impedance, the effects on the reflection coefficient (S_{11}) of the rectenna caused by the impedance variation of the nonlinear elements (rectifying diodes) may not be very significant. Therefore, compared with the conventional 50 Ω (low impedance) matching system, the nonlinear effects of the rectenna can be significantly reduced by using this new configuration. The rectenna may have a good performance in a range of operating conditions such as different input power levels, different load values, or even different types of rectifying diodes. In addition, the proposed rectenna configuration can reduce the total cost and avoid fabrication errors due to its very simple structure.

III. HIGH IMPEDANCE ANTENNA DESIGN

A. Off-Center-Fed Dipole Theory

There have been various types of high impedance antenna reported in the literature [28], [29], but none of them can provide a constantly high impedance over a wide frequency range which is very important for realizing the proposed broadband high-efficiency rectenna. There are no available approaches that can tune the antenna impedance over a wide frequency band to the desired values. Consequently, if these high impedance antennas were used without matching networks, the bandwidth of the rectenna could become very narrow.

Here, we propose a broadband high impedance antenna, the off-center-fed dipole (OCFD) antenna.

As depicted in Fig. 3, the OCFD antenna is different from a conventional center-fed symmetrical dipole antenna, where the two dipole arms are asymmetrical and have unequal lengths. The typical application of the OCFD is to realize a multiband antenna, since the resonant center-fed d has its fundamental frequency at f_0 and harmonics at $3f_0$, $5f_0$, $7f_0$, and so on. While the OCFD can resonate at f_0, $2f_0$, $4f_0$, and $8f_0$ by offsetting the feed by λ/4 from the center [30]. Such OCFDs are very popular in the amateur radio community. Recently, some researchers used the OCFD to create a 90° phase delay and generate circular polarization radiation field for the antenna [31]. But, one of the major problems of the OCFD is that the radiation resistance of the antenna could be very high; thus, it is required to use a 4:1 or 6:1 balun transformer to convert the impedance to the feeding port 50 Ω resistance [32]. This is a disadvantage for most of those applications using OCFDs (in a conventional 50 Ω feed system), but we may take advantage of this feature in the proposed rectenna design. The OCFD antenna may be well matched to a rectifier without using matching networks since the rectifiers are normally of high input impedance as well. We assume a half-wavelength center-fed dipole and an OCFD having the same total length and radiating the same power, as shown in Fig. 3. The currents at the feed points for the symmetrical and asymmetrical dipoles are I_S and I_{AS}, respectively. From [38], the relationship between the currents can be expressed as

$$I_{\mathrm{AS}} = I_S \sin\alpha \tag{1}$$

where α is the measured angle from one end in electrical degrees (between 0 and π as shown in Fig. 3). Thus, the power radiated by both antennas can be calculated as

$$P_S = I_S^2 R_S \tag{2}$$

$$P_{\mathrm{AS}} = I_{\mathrm{AS}}^2 R_{\mathrm{AS}} \tag{3}$$

where R_S and R_{AS} are the radiation resistances of the center-fed dipole and the OCFD, respectively. Since we have assumed $P_S = P_{\mathrm{AS}}$, thus we can obtain

$$\frac{R_S}{R_{\mathrm{AS}}} = \frac{I_{\mathrm{AS}}^2}{I_S^2}. \tag{4}$$

Using (1), the relationship between the radiation resistances R_S and R_{AS} can be written as

$$R_S = \frac{R_{\mathrm{AS}}}{(\sin\alpha)^2}. \tag{5}$$

Thus, when $\alpha = 90^\circ$ or ($\pi/2$), the dipole is center-fed since $\sin\alpha = 1$ and $R_S = R_{\mathrm{AS}}$. It is demonstrated that the value of R_{AS} is always larger than the value of R_{S} if the dipole is off-center-fed. In addition, we could tune the radiation resistance of the OCFD to a desired value by changing the value of $\sin\alpha$ (position of the feed point).

In order to gain a better understanding, we study a simple OCFD antenna in free space with the aid of the CST software. Assume that the arms of the dipole are made by perfect electric conductor wires with a diameter of 1 mm. The total length of the OCFD is 100 mm while the feeding port separation is 1 mm. If the antenna is considered as a typical half-wavelength dipole, then the fundamental frequency should be about 1.5 GHz. The computed real part and imaginary part of the input impedance of the OCFD at 1.5 GHz are given in Table I for different feed locations. As can be seen from the table, the radiation resistance of the dipole is 73 Ω when the two arms have the same length. By changing the feed position, the radiation resistance can be

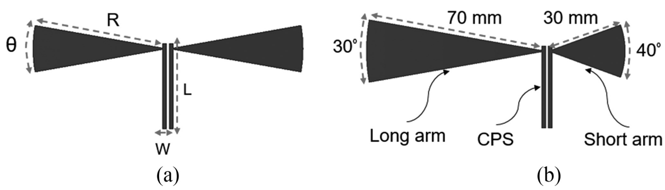

Fig. 4. (a) The broadband center-fed symmetrical dipole antenna. (b) The broadband off-center-fed dipole antenna.

increased where the value is about 320 Ω for the long arm being 90 mm and the short arm being 10 mm. Compared with the impedance of a symmetrical dipole (73 Ω), the OCFD has increased the impedance value up to 4.4 times. The imaginary part of the input impedance is around 0–6 Ω and the ratio of the long arm over the short arm is less than 7/3. Therefore, if the symmetrical dipole is of a broad bandwidth, the OCFD may produce constantly high impedance over the bandwidth of interest.

B. Broadband OCFD Antenna Design

A broadband center-fed symmetrical dipole is proposed as the starting point to design a broadband OCFD antenna. As shown in Fig. 4(a), the arms of the dipole are shaped as radial (bowtie) stubs to broaden the frequency bandwidth. The bowtie dipole antenna is a planar version of a biconical antenna. From [36], the characteristic impedance (Z_k) of an infinite biconical antenna is given by

$$Z_k = 120 \text{ In } \cot(\theta/4) \tag{6}$$

where θ is the cone angle. Then, the input impedance (Z_i) of the biconical antenna with a finite length can be written as

$$Z_i = Z_k \frac{Z_k + jZ_m \tan \beta l}{Z_m + jZ_K \tan \beta l} \tag{7}$$

where $\beta = 2\pi/\lambda$ (λ is the wavelength), l = cone length, and $Z_m = R_m + j\,X_m$. While the values of R_m and X_m are given by Schellkunoff [37] for a thin biconical antenna ($\theta < 5°$). As indicated in [36], the VSWR of the biconical antenna can be less than 2 over a 2:1 bandwidth. Meanwhile, the input impedance of the bowtie dipole is similar to that of the biconical antenna, where the value of the impedance is a function of frequency, length of the arm (*R*), and cone angle (θ).

The aforementioned theories could be utilized to predict the initial performance (such as the frequency bandwidth) of this broadband antenna with a given dimension. But the actual performance might be varied in the simulation and measurement due to the practical configuration of the antenna (e.g., effects of PCB and feed). Therefore, in order to maintain the antenna performance, the major design parameters of the antenna should be further tuned using the software. As a design guide, the parametric effects (values of the *R* and θ) on the frequency bandwidth of the bowtie dipole [as shown in Fig. 4(a)] are studied. If the antenna is printed on a Rogers RT6002 board with a relative permittivity of 2.94 and a thickness of 1.52 mm, it is fed by a pair of coplanar striplines (CPS) where the length (*L*) of each strip is 32 mm and the width (*W*) is 1.5 mm. The gap between the CPS is 1 mm. The antenna is modeled using the CST software. The simulated frequency bandwidth (for VSWR <2 with 50 Ω port) of the bowtie dipole is shown in Table II for different cone angles and lengths of the arm.

TABLE II
SIMULATED FREQUENCY BANDWIDTH OF THE BOWTIE DIPOLE

	$R = 40$ mm	$R = 50$ mm	$R = 60$ mm
$\theta = 10°$	1.93–2.14 GHz	1.83–1.93 GHz	1.58–1.97 GHz
$\theta = 30°$	1.93–2.28 GHz	1.75–2.17 GHz	1.58–1.98 GHz
$\theta = 50°$	1.91–2.25 GHz	1.73–2.19 GHz	1.55–2 GHz
$\theta = 70°$	1.91–2.28 GHz	1.73–2.21 GHz	1.55–2.03 GHz

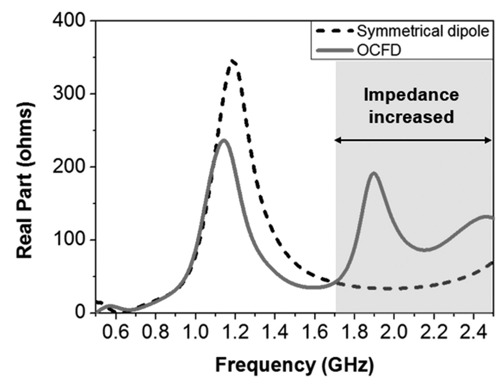

Fig. 5. Simulated real part of the impedance of the symmetrical dipole and the OCFD.

From the results in Table II, it can be seen that the bowtie symmetrical dipole is indeed of a broad bandwidth. Moreover, the antenna could have a larger frequency bandwidth for larger cone angles, and have a lower resonant frequency band for larger dimensions (length of the arm). In this work, we select $R = 50$ mm and $\theta = 30°$ as an example, since the frequency band (from 1.75 to 2.17 GHz) has covered some popular mobile frequency bands such as the GSM1800 and UMTS2100. Hence, the arms of the symmetrical bowtie dipole have a radius of 50 mm and an angle of 30° for the radial stub structure. The maximum total length of the complete dipole antenna is about 100 mm.

To design the OCFD, the length of the longer arm is increased to 70 mm while the length of the shorter arm is, therefore, reduced to 30 mm. In addition, in order to enhance asymmetry between the arms, the circumference angle of the shorter arm is increased to 40°. The total length of the dipole is still of around 100 mm, as shown in Fig. 4(b). But the ratio of the long arm to the short arm has been changed from 5/5 to 7/3. In this scenario, the real part of the impedance over the frequency band may be increased while the imaginary part could be maintained over the resonant frequency band (as discussed in Table I). Fig. 5 shows the simulated real part of the input impedance of the symmetrical dipole and the OCFD. It can be seen that the impedance of the symmetrical dipole is around 50 Ω for frequencies between 1.75 and 2.4 GHz (around the 2nd and 3rd resonant frequency bands), which verifies the broadband per-

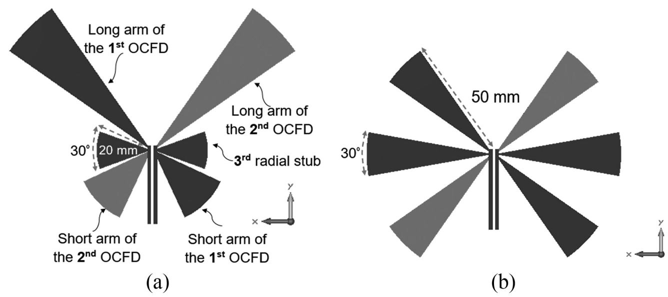

Fig. 6. (a) The proposed crossed off-center-fed dipole antenna. (b) The reference antenna with symmetrical arms for performance comparison.

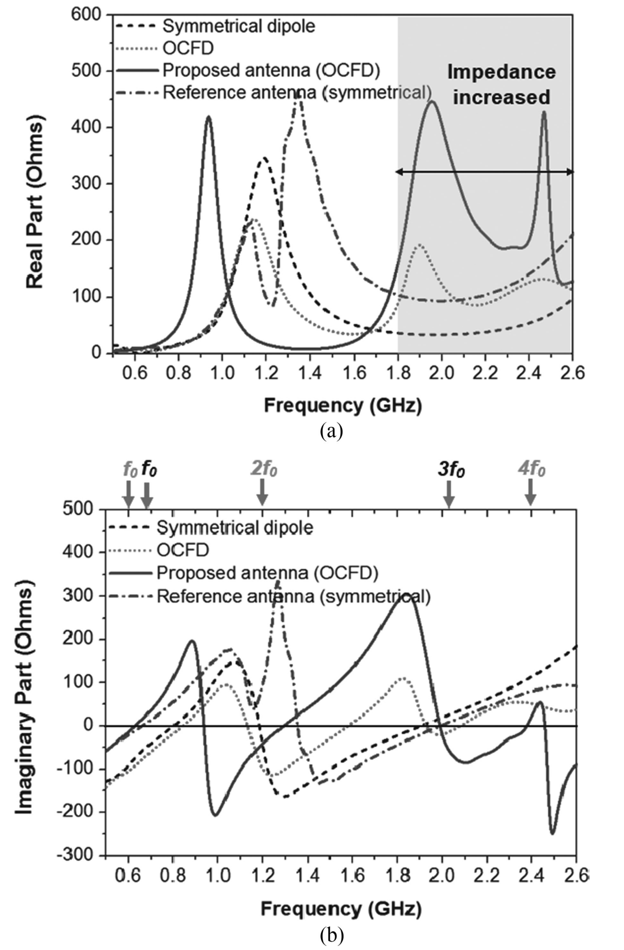

Fig. 7. Simulated input impedance of four different antennas. (a) Real part. (b) Imaginary part.

formance of the antenna as depicted in Table II. However, the impedance of the OCFD is from 100 to 200 Ω over the frequency band between 1.8 and 2.5 GHz, which is much higher than that of the symmetrical dipole. It is shown that, by modifying a broadband symmetrical bowtie dipole to an OCFD, the antenna impedance is significantly increased over the desired resonant frequency range. In addition, the impedance for both antennas at the frequencies from 1.1 to 1.2 GHz is also very high (i.e., over 200 Ω), this is due to the antiresonance of the dipole antenna [31].

The next step is to modify the proposed OCFD to a crossed OCFD by introducing another OCFD. As shown in Fig. 6(a), the second OCFD (red) has the same dimensions as the first one, but they are orthogonal to each other. The purpose is to achieve dual polarization receiving capability and generate a vertically symmetrical radiation pattern for the antenna. Finally, another pair of radial stubs (blue) is inserted between the two OCFDs to further manipulate the impedance. The final antenna layout is show in Fig. 6(a) which looks symmetrical from left to right as a whole. For comparison, a reference antenna consisting of three dipoles with symmetrical arms is studied. As shown in Fig. 6(b), the arms of the reference antenna have a radius of 50 mm and a circumference angle of 30° for the radial stub. Thus, the reference antenna and the proposed antenna have the same electrical length (100 mm). The simulated real part and imaginary part of the input impedance of four different antennas (single symmetrical dipole, single OCFD, proposed OCFD, and reference antenna) are shown in Fig. 7(a) and (b). It can be seen that the real part of the input impedance of the proposed broadband OCFD antenna is above 180 Ω (up to 450 Ω) for the frequency band between 1.8 and 2.5 GHz, which is much higher than that of the reference antenna (around 100 Ω). In addition, the proposed antenna has shifted the high-impedance (about 400 Ω) frequency from around 1.4 to around 0.9 GHz. This is likely due to the coupling effects among the three dipoles. The imaginary part of the reference antenna is around 0 Ω at frequencies around 0.7 and 2.1 GHz, which are f_0 and $3f_0$, respectively. While the imaginary part of the proposed OCFD is around 0 Ω at resonant frequencies 0.6, 1.2, and 2.4 GHz, which are f_0, $2f_0$, and $4f_0$, respectively. These results have demonstrated that the simulated results agree with the OCFD theory as discussed in Section III-A. Furthermore, the imaginary part of the impedance of the antenna over the resonant frequency band from 1.4 to 2 GHz turns from negative values (for the reference antenna) to positive values (for the proposed antenna). As shown in Fig. 7(b), the value of the imaginary part of the proposed antenna impedance varies between 0 and 300 Ω over the desired frequency band. This feature could help the proposed antenna to produce a better conjugate matching with the rectifier, since the imaginary part of the impedance of the rectifier normally varies between –700 and 0 Ω as we discussed earlier. The simulated three dimensional (3-D) radiation patterns of the proposed antenna at the frequencies of interest are depicted in Fig. 8. The two-dimensional (2-D) polar plots of antenna patterns in *E-plane* and *H-plane* are shown as well. Here, we have only showed the directivity (maximum gain) of the antenna (without taking the mismatch loss into account). From Fig. 8, it can be seen that the antenna has symmetrical patterns about YOZ plane with a maximum directivity of 1.8 dBi at 0.9 GHz, 3.5 dBi at 1.8 GHz, and 3.3 dBi at 2.4 GHz. The antenna is more directive toward the long arm direction at 1.8 and 2.4 GHz with the half-power beam-widths (HPBW) of around 174° and 185°, respectively. The HPBW is about 96° at 0.9 GHz.

Therefore, the proposed broadband OCFD antenna has obtained high impedance over a wide frequency range. The

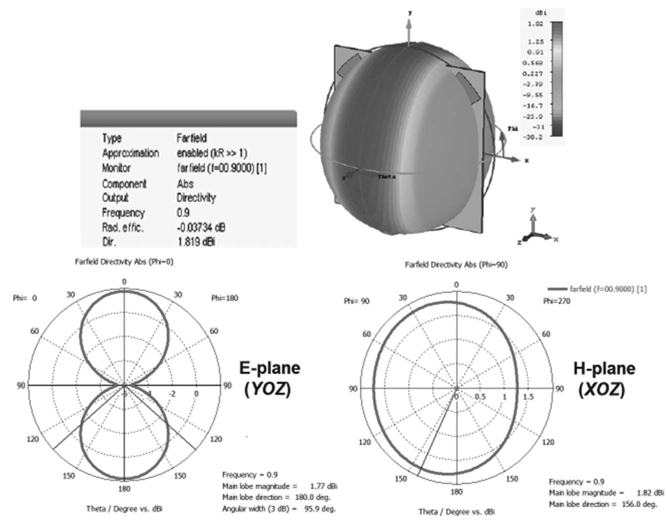

(a)

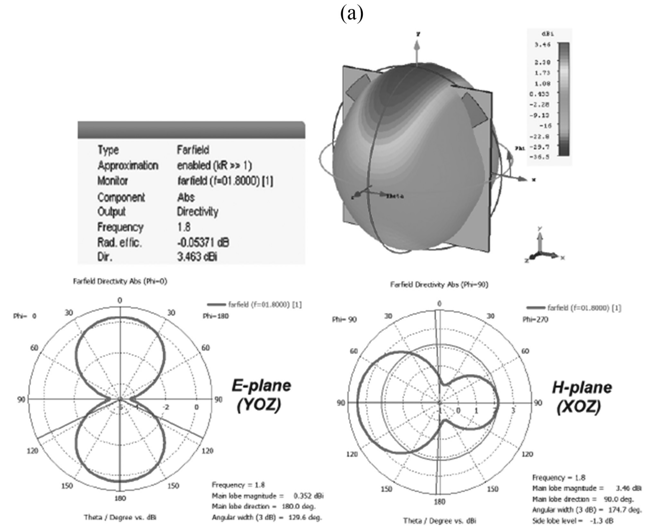

(b)

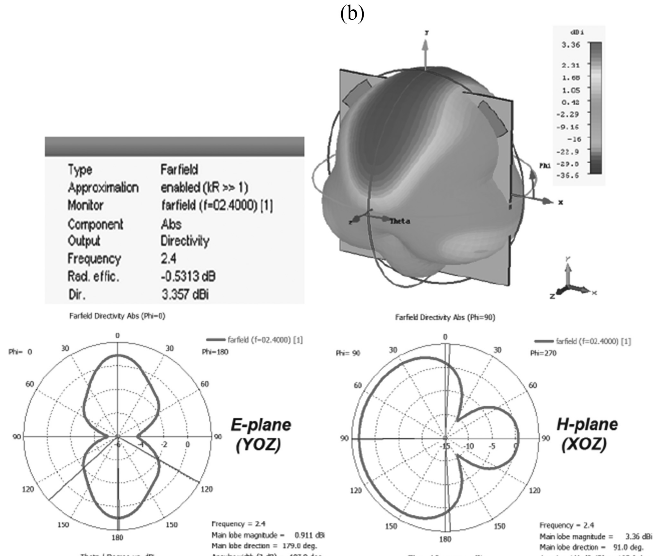

(c)

Fig. 8. Simulated 3-D patterns with directivities and 2-D patterns over *E*-plane and *H*-plane of the proposed antenna at (a) 0.9 GHz, (b) 1.8 GHz, and (c) 2.4 GHz.

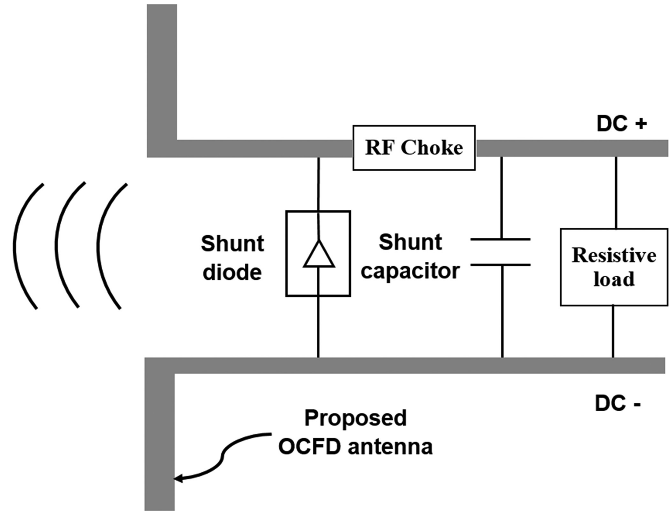

Fig. 9. Configuration of a single shunt diode (Class F) rectifier with a dipole antenna.

proposed design is just an example to illustrate the proposed new method. The details of the dipole could be modified according to the frequency of interest.

IV. Rectenna Integration

A. Rectifier Configuration

The proposed high impedance OCFD antenna may directly conjugate match with the input impedance of a rectifier over a wide frequency band. The rectifier should only consist of few circuit components for rectification, dc storage, and output. A single shunt diode rectifier is selected due to its very simple structure and high conversion efficiency [33]. The configuration of the single shunt diode rectifier with a dipole antenna is depicted in Fig. 9. The shunt diode is used as the rectifying element and the diodes for high frequency (e.g., $f > 1$ GHz) applications are normally Schottky diodes such as SMS7630 (from Skyworks) and HSMS2860 (from Avago). A shunt capacitor after the diode is used to store dc power and smooth the dc output waveforms. In addition, a series connected RF choke is placed between the diode and capacitor to block ac components generated from the diode. In this design, a typical inductor of 47 nH is selected as the RF choke. To have a better configuration on the PCB, the proposed antenna and rectifier are both fed by CPS (or twin-wire conducting strips). The topology of the rectifier configured with the conducting strips extended from the OCFD antenna is shown in Fig. 10. The values and part numbers of the circuit components are given in Table III.

The rectifier is built and simulated by using the ADS software. To improve the accuracy of results, the diode is modeled by using a nonlinear SPICE model with parasitic elements provided by the suppliers (such as Skyworks). The chip inductor and capacitor are modeled by using the real product models, including the *S*-parameter files, provided by Murata and Coilcraft. Since the proposed design can eliminate the matching network between the antenna and the rectifier, thus the rectifying circuit

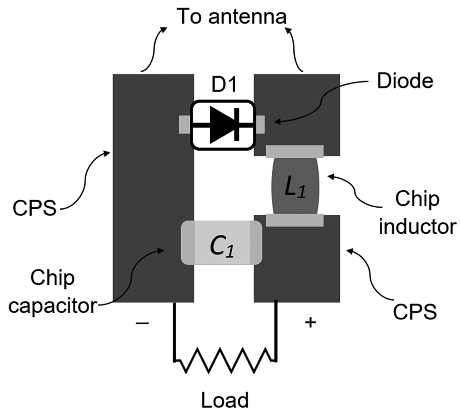

Fig. 10. Configuration of the proposed rectifier on coplanar striplines (CPS).

TABLE III
CIRCUIT COMPONENTS USED IN THE DESIGN

Component name	Nominal Value	Part number and supplier
D1	Schottky diode	SMS7630-079LF, Skyworks
L1	47 nH chip inductor	0603HP47N, Coilcraft
C1	100 nF chip capacitor	GRM188R71H104JA93D, Murata

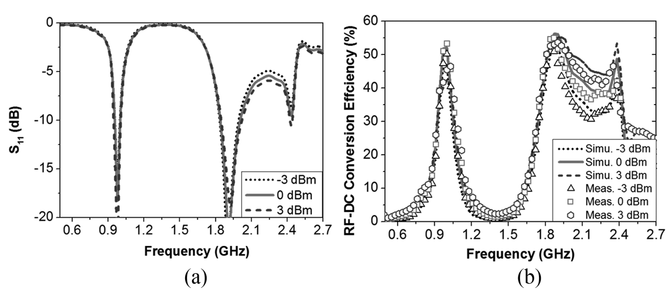

Fig. 11. (a) The simulated S_{11} and (b) the simulated and measured RF–dc conversion efficiency of the rectenna at three different input power levels. The load resistance is 400 Ω.

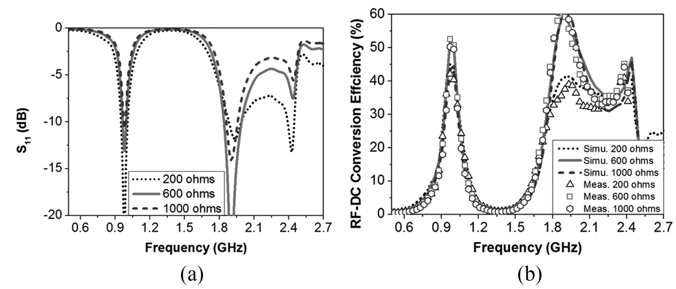

Fig. 12. (a) The simulated S_{11} and (b) the simulated and measured RF–dc conversion efficiency of the rectenna at three different load values. The input power level is 0 dBm.

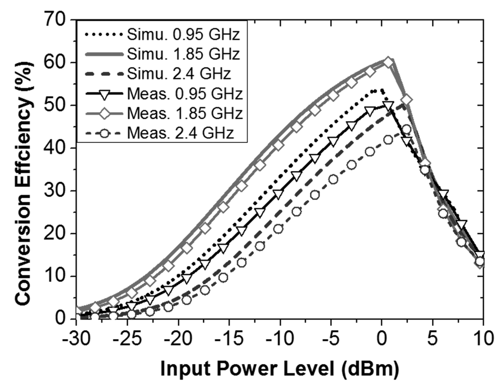

Fig. 13. Simulated and measured conversion efficiency of the rectenna versus input power level at three frequencies. The load resistance is 600 Ω.

is indeed simplified. The frequency domain power source port is used in the simulation, and the port impedance is defined as the impedance of the proposed OCFD antenna by using the touchstone S1P files exported from the CST, similarly to the results shown in Fig. 7(a) and (b).

B. Rectenna Performance

After the complete rectenna has been designed, its performance is evaluated by using the harmonic balance simulation and the large signal *S*-parameter simulation using the ADS. The performances of the proposed rectenna in terms of the reflection coefficient (S_{11}) and RF–dc conversion efficiency are shown in Figs. 11–13. The RF–dc conversion efficiency is obtained by

$$\eta_{\mathrm{RF-dc}} = \frac{P_{\mathrm{dc}}}{P_{\mathrm{in}}} \tag{8}$$

where P_{dc} is the output dc power and *Pin* is the input RF power to the antenna. S_{11} (simulated) and conversion efficiency (simulated and measured) of the rectenna at different input power levels are shown in Fig. 11(a) and (b) as a function of frequency. A typical load resistor of 400 Ω is selected. From Fig. 11, it can be seen that the rectenna covers the desired broad frequency band from 1.8 to 2.5 GHz and an additional frequency band around 1 GHz. The S_{11} of the rectenna is lower than –10 dB between 1.8 and 2 GHz and around 1 GHz. The conversion efficiency is higher than 40% (up to 55%) over the entire frequency band of interest for the input power level of 0 dBm (1 mW). In addition, when the input power is doubled (3 dBm) or halved (–3 dBm), the reflection coefficients are always smaller than –6 dB from 1.8 to 2.5 GHz, while the efficiency over the band of interest is still high (e.g., greater than 35%).

Fig. 12(a) and (b) depicts the S_{11} (simulated) and conversion efficiency (simulated and measured) of the rectenna for different load values. It can be seen that the efficiency is higher than 30% (up to 60%) for the load values from 200 to 1000 Ω and for the frequencies between 1.8 and 2.5 and the around 1 GHz. It is demonstrated that the nonlinear effects linked to the input power and load are reduced in the proposed broadband rectenna, which verifies our predictions in Section II. The simulated and measured conversion efficiency of the rectenna versus input power level is shown in Fig. 13 at three frequencies. It can be seen that the rectenna has the highest efficiency at the input

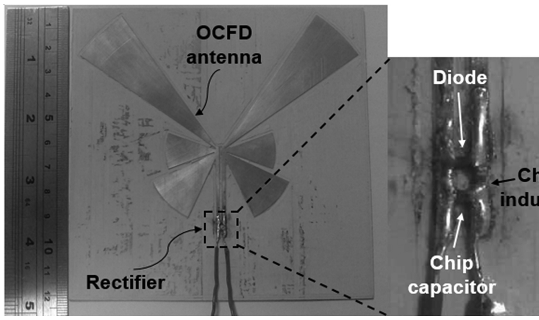

Fig. 14. Fabricated prototype rectenna. The enlarged view of the rectifier is shown as well.

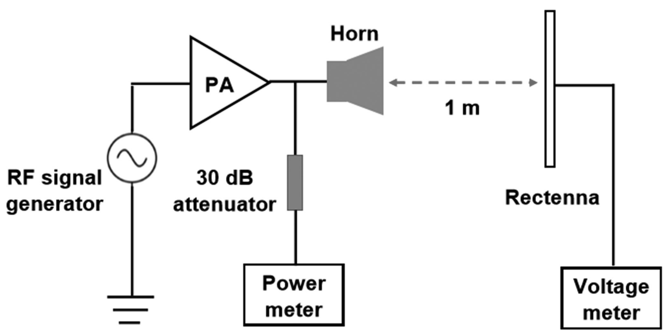

Fig. 15. Measurement setup of the rectenna.

power of around 0 dBm. This is because the selected diode (SMS7630) has reached its reverse breakdown voltage. Since this diode has a very low forward bias voltage (150 mV) and a low breakdown voltage (2 V) [34], it is normally applied in low input power (e.g., from –30 to 0 dBm) applications. For high input power applications (e.g., >10 dBm) and higher conversion efficiency (e.g., up to 80%), other diodes with a higher breakdown voltage could be selected.

V. Rectenna Measurements and Validations

The fabricated prototype rectenna is shown in Fig. 14 and the measurement setup is depicted in Fig. 15. Since the proposed antenna has been integrated with the rectifier, S_{11} of the rectenna cannot be measured directly. A standard horn antenna R&SHF906 was used to transmit the RF power. A 30 dB gain PA amplifies the signal generated by an RF signal generator (Keithley2920). The rectenna was configured to receive the signal at a distance of 1 m (in antenna far field). The output dc voltage (V_{dc}) was measured by using a voltage meter and the output dc power can be obtained by using $P_{\mathrm{out}} = V_{\mathrm{dc}}^2/R$, where R is the load resistance.

The available power to the transmitting horn antenna was measured by using a power meter; thus, the received RF power by the rectenna can be estimated by using the Friis transmission equation [35]

$$P_r = P_t + G_t + G_r + 20\log_{10}\frac{\lambda}{4\pi r} \tag{9}$$

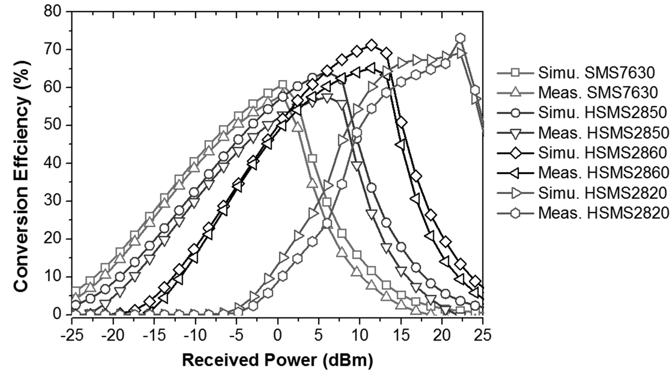

Fig. 16. Simulated and measured conversion efficiency of the rectenna versus input power level for using different types of Schottky diodes. The frequency is 1.85 GHz.

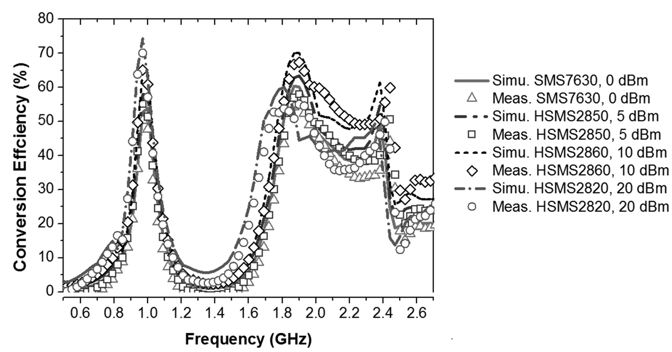

Fig. 17. Simulated and measured conversion efficiency of the rectenna versus frequency for using different types of Schottky diodes at the optimal input power levels. The load resistance is 500 Ω.

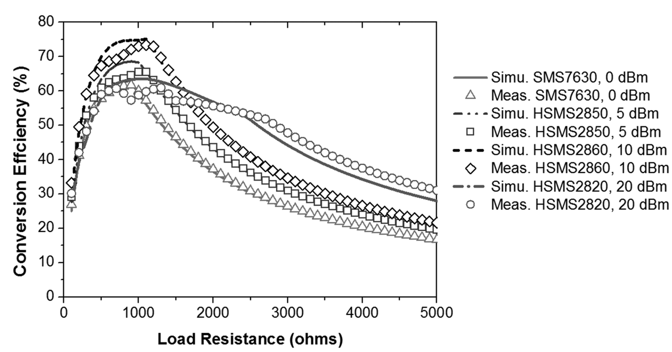

Fig. 18. Simulated and measured conversion efficiency of the rectenna versus load resistance for using different types of Schottky diodes at the optimal input power levels. The frequency is 1.85 GHz.

where P_r is the received power in dBm, P_t is the power obtained from the power meter in dBm, *Gt* is the realized gain of the transmitting antenna in dB, *Gr* is the realized gain of the receiving antenna (rectenna) in dB, λ is the wavelength, and r is the distance between the TX and RX antennas ($r = 1$ m).

As discussed earlier, the proposed rectenna can reduce the effects of the nonlinearity of the rectifier and match well to a wide range of load impedance values. Thus, the rectenna may perform well even when different types of diodes are used.

TABLE IV
RECTENNA PERFORMANCE FOR USING DIFFERENT DIODES

Schottky diodes name	Simulated input impedance under the same condition (Ω)	Optimal input power level	Maximum conversion efficiency	Optimal load resistance range (Ω)
SMS7630	173 – *j* 36	0 dBm	60%	250–1500
HSMS2850	325 – *j* 57	5 dBm	65%	200–2000
HSMS2860	349 – *j* 166	10 dBm	70%	200–2500
HSMS2820	82 – *j* 145	20 dBm	75%	250–3000

This advantage is normally not available in the conventional rectenna designs, since the input impedance and characteristics of the diodes can be very different. Thus, in order to validate this point, the proposed rectenna was measured by using different types of Schottky diodes such as HSMS2850, HSMS2860, and HSMS2820. The measured conversion efficiency versus input power level is shown in Fig. 16 along with simulated results. High conversion efficiency is obtained in all cases. When the load is selected as 500 Ω and the frequency is selected as 1.85 GHz, we have $Gt = 8.5\,\mathrm{dBi}$, $Gr = 3.45\,\mathrm{dBi}$, $\lambda = 0.162\,\mathrm{m}$, and $r = 1\,\mathrm{m}$. Using (9), the correlation between the transmitting power and the receiving power can be obtained as

$$\mathrm{Pr}\,(\mathrm{dBm}) = \mathrm{Pt}\,(\mathrm{dBm}) - 25.84\ \mathrm{dB}. \qquad (10)$$

It can be seen that the maximum conversion efficiency and the corresponding input powers of the rectenna are 60% at 0 dBm, 65% at 5 dBm, 70% at 10 dBm, and 75% at 20 dBm for using the Schottky diodes SMS7630, HSMS2850, HSMS2860, and HSMS2820, respectively. The peak efficiency is realized at different input power levels. This is because the breakdown voltages for the selected diodes are different, which are 2 V (SMS7630), 3.8 V (HSMS2850), 7 V (HSMS2860), and 15 V (HSMS2820), respectively. The efficiency is much higher at high input power levels for using the diodes with large breakdown voltages (e.g., HSMS2820), while the efficiency is higher at low input power levels for using the diodes with small forward bias voltages (e.g., SMS7630). The simulated and measured conversion efficiencies of the rectenna (using the four different diodes) are depicted in Fig. 17 as a function of the frequency. The load is still 500 Ω while the input power levels are selected as the optimal input powers for these diodes (e.g., 0 dBm for SMS7630, 5 dBm for HSMS2850, 10 dBm for HSMS2860, and 20 dBm for HSMS2820). Note that in the measurements, the correlation between the transmitting power and the receiving power [as given in (9)] might be changed if the frequencies are different. Thus, the transmitting power should be tuned to make sure that the received power is approximately a constant value in the broadband (e.g., 0 dBm for the frequencies from 0.9 to 3 GHz).

From the results in Fig. 17, it can be seen that the rectenna is still of broadband performance (1.8 to 2.5 GHz) when using different diodes, and the conversion efficiency is constantly high over the frequency bandwidth of interest for the selected input power levels. Figs. 16 and 17 show a good agreement between the simulated and measured results.

Fig. 18 shows the simulated and measured conversion efficiency by using different load resistances. The frequency is selected as 1.85 GHz while the input power levels are still set as the optimal input powers. In reality, the load impedance may vary over a large range in different applications; thus, it is important to reduce the sensitivity of efficiency versus load variation in a nonlinear system (rectenna). From Fig. 18, it can be seen that, when using different diodes, the efficiency of the rectenna is constantly high (from 40% to 75%) for the load values between 200 and 2000 Ω, then the efficiency starts to decease due to the impedance mismatch between the antenna and the rectifier. It demonstrates that the nonlinear effects have been reduced over the load range from 200 to 2000 Ω. For other load values, the details of the rectenna can be modified to achieve good performance.

According to the results in Figs. 16–18, the performance of the rectenna by using different diodes is summarized in Table IV. The simulated input impedance of the rectifier is shown under the same condition (frequency: 1.85 GHz, input power: 10 dBm, and load: 500 Ω). The impedance is very different for different types of diodes, but our rectenna can still be well configured with these diodes without using matching networks. It is demonstrated that the proposed broadband rectenna can work well under different operating conditions. The nonlinear effects have been reduced. The matching networks have indeed been eliminated. In addition, the optimal input power level of the device is tunable (from 0 to 23 dBm) by selecting appropriate diodes so that the conversion efficiency of the broadband rectenna can be always higher than 60% (as shown in Fig. 16). This is very important for WPT or WEH used in practice.

A comparison between our rectennna and other related work is shown in Table V. It can be seen that our design seems to be the only one without using the matching networks, but still achieves high conversion efficiency over a relatively wide frequency band. The conversion efficiency of our design is comparable with that of the other work used matching networks, while the performance of the rectenna is reasonably well in a range of input powers and load impedance. In addition, our device is also the only one which can use different types of diodes without changing any other part of the circuit. The structure of our design is the simplest for broadband rectennas with similar performance. The proposed rectenna is of good industrial value due to its simplicity and universality, and is of good practical value due to its consistent performance under different operating conditions.

Also, the proposed concept for eliminating the matching networks is not just limited in the presented design, and can also be used in other similar nonlinear systems.

TABLE V
COMPARISON OF THE PROPOSED RECTENNA AND RELATED DESIGNS

Ref. (year)	Frequency (GHz)	Use of impedance matching networks	Complexity of the overall design	Maximum conversion efficiency (%)	Input power level for conversion efficiency > 60%	Optimal load range with good performance (kΩ)	Type of Schottky diode
[18] (2015)	Four-band 0.9, 1.8, 2.1, 2.4	Yes	Very complex	65 at 0 dBm	–5 to 0 dBm	11	MSS20-141
[19] (2015)	Broad-band 1.8–2.5	Yes	Complex	70 at 0 dBm	–7 to 0 dBm	14.7	SMS7630
[20] (2015)	Dual-band 0.915, 2.45	Yes	Complex	70 at 0 dBm	–5 to 0 dBm	0.5–3	SMS7630
[23] (2012)	Tunable 0.9–2.45	Yes	Very complex	80 at 30 dBm	Tunable 5 to 30 dBm	1–4	Tunable
[24] (2016)	Six-band 0.55, 0.75, 0.9, 1.85, 2.15, 2.45	Yes	Very complex	68 at –5 dBm	–5 to 0 dBm	10–75	SMS7630
[25] (2012)	Single-band 2.45	No	Simple	70 at –5 dBm	–10 to 5 dBm	2.8	HSMS2852
[26] (2004)	Broad-band 2–18	No	Medium	20 at 17 dBm	Not available	0.6	SMS7630
This work (2016)	**Broad-band 0.9–1.1, 1.8–2.5**	**No**	**Simplest**	**75 at 20 dBm**	**Tunable 0 to 23 dBm**	0.2–2	**Tunable**

VI. CONCLUSION

A novel method for eliminating the matching network of broadband rectennas was presented. An OCFD antenna was designed, where the antenna impedance was tuned to directly match with the rectifier. The proposed rectenna was of a broad bandwidth and high efficiency, and had excellent performance under different operating conditions. The measured performance showed that the operating frequencies of the experimental rectenna were from 0.9 to 1.1 GHz and from 1.8 to 2.5 GHz (which were the typical cellular mobile, WLAN, and ISM bands), while the maximum conversion efficiency was up to 75% and the optimal input power range was tunable from 0 to 23 dBm by selecting appropriate diodes. In addition, the rectenna had a very simple structure and low cost. Considering the excellent overall performance of the proposed rectenna, it is suitable for high efficiency WPT and WEH applications. The design concept is easy to follow while its details can be optimized for different applications.

ACKNOWLEDGMENT

The authors would like to thank the anonymous reviewers for their constructive feedback of this paper. The authors would also like to thank Prof. S. Hall from the University of Liverpool for the refinement of the manuscript.

REFERENCES

[1] S. Carreon-Bautista, A. Eladawy, A. N. Mohieldin, and E. Sanchez-Sinencio, “Boost converter with dynamic input impedance matching for energy harvesting with multi-array thermoelectric generators,” *IEEE Trans. Ind. Electron.*, vol. 61, no. 10, pp. 5345–5353, Oct. 2014.

[2] J. Jeong and D. Jang, “Design technique for harmonic-tuned RF power oscillators for high-efficiency operation,” *IEEE Trans. Ind. Electron.*, vol. 62, no. 1, pp. 221–228, Jan. 2015.

[3] J. Kim, D.-H. Kim, and Y.-J. Park, “Analysis of capacitive impedance matching networks for simultaneous wireless power transfer to multiple devices,” *IEEE Trans. Ind. Electron.*, vol. 62, no. 5, pp. 2807–2813, May 2015.

[4] K. Song and Q. Xue, “Ultra-wideband ring-cavity multiple-way parallel power divider,” *IEEE Trans. Ind. Electron.*, vol. 60, no. 10, pp. 4737–4745, Oct. 2013

[5] K. Rawat and F. M. Ghannouchi, “Design methodology for dual-band Doherty power amplifier with performance enhancement using dualband offset lines,” *IEEE Trans. Ind. Electron.*, vol. 59, no. 12, pp. 4831–4842, Dec. 2012

[6] X. Wang, X. K. Guan, and S. Q. Fan, “ESD-protected power amplifier design in CMOS for highly reliable RFICs,” *IEEE Trans. Ind. Electron.*, vol. 58, no. 7, pp. 2736–2743, Jun. 2011.

[7] R. Johari, J. V. Krogmeier, and D. J. Love, “Analysis and practical considerations in implementing multiple transmitters for wireless power transfer via coupled magnetic resonance,” *IEEE Trans. Ind. Electron.*, vol. 61, no. 4, pp. 1174–1183, Apr. 2014.

[8] L. Chen, Y. C. Zhou, and T. J. Cui, “An optimizable circuit structure for high-efficiency wireless power transfer,” *IEEE Trans. Ind. Electron.*, vol. 60, no. 1, pp. 339–349, Jan. 2013.

[9] H. J. Visser and R. J. M. Vullers, “RF energy harvesting and transport for wireless sensor network applications: Principles and requirements,” *Proc. IEEE*, vol. 101, no. 6, pp. 1410–1423, Jun. 2013.

[10] S. Cheon, Y.-H. Kim, S.-Y. Kang, M. L. Lee, J.-M. Lee, and T. Zyung, “Circuit-model-based analysis of a wireless energy-transfer system via coupled magnetic resonances,” *IEEE Trans. Ind. Electron.*, vol. 58, no. 7, pp. 2906–2914, Jul. 2011.

[11] J. Colomer-Farrarons, P. Miribel-Català, A. Saiz-Vela, and J. Samitier, “A multiharvested self-powered system in a low-voltage low-power technology,” *IEEE Trans. Ind. Electron.*, vol. 58, no. 9, pp. 4250–4263, Sep. 2011.

[12] Y. Huang, N. Shinohara, and T. Mitani, “A constant efficiency of rectifying circuit in an extremely wide load range,” *IEEE Trans. Microw. Theory Techn.*, vol. 62, no. 4, pp. 986–993, Apr. 2014.

[13] P. Lu, X. Yang, J. Li, and B. Wang, “A compact frequency reconfigurable rectenna for 5.2- and 5.8-GHz wireless power transmission,” *IEEE Trans. Power Electron.*, vol. 30, no. 11, pp. 6006–6010, Nov. 2015.

[14] J. O. McSpadden, F. Lu, and K. Chang, “Design and experiments of a high conversion efficiency 5.8-GHz rectenna,” *IEEE Trans. Microw. Theory Techn.*, vol. 46, no. 12, pp. 2053–2060, Dec. 1998.

[15] H. Sun, Y.-X. Guo, M. He, and Z. Zhong, “A dual-band rectenna using broadband Yagi antenna array for ambient RF power harvesting,” *IEEE Antennas Wireless Propag. Lett.*, vol. 12, pp. 918–921, 2013.

[16] K. Niotaki, S. Kim, S. Jeong, A. Collado, A. Georgiadis, and M. Tentzeris, “A compact dual-band rectenna using slot-loaded dual band folded dipole antenna,” *IEEE Antennas Wireless Propag. Lett.*, vol. 12, pp. 1634–1637, 2013.

[17] R. Scheeler, S. Korhummel, and Z. Popovic, “A dual-frequency ultralow-power efficient 0.5-g rectenna,” *IEEE Microw. Mag.*, vol. 15, no. 1, pp. 109–114, Jan. 2014.

[18] V. Kuhn, C. Lahuec, F. Seguin, and C. Person, “A multi-band stacked RF energy harvester with rf-to-dc efficiency up to 84%,” *IEEE Trans. Microw. Theory Techn.*, vol. 63, no. 5, pp. 1768–1778, May 2015.

[19] C. Song, Y. Huang, J. Zhou, J. Zhang, S. Yuan, and P. Carter, “A high-efficiency broadband rectenna for ambient wireless energy harvesting,” *IEEE Trans. Antennas Propag.*, vol. 63, no. 8, pp. 3486–3495, May 2015.

[20] K. Niotaki, A. Georgiadis, A. Collado, and J. S. Vardakas, “Dual-band resistance compression networks for improved rectifier performance,” *IEEE Trans. Microw. Theory Techn.*, vol. 62, no. 12, pp. 3512–3521, Nov. 2015.

[21] Y. Han, O. Leitermann, D. A. Jackson, J. M. Rivas, and D. J. Perreault, “Resistance compression networks for radio-frequency power conversion,” *IEEE Trans. Power Electron.*, vol. 22, no. 1, pp. 41–53, Jan. 2007.

[22] T. Paing, J. Shin, R. Zane, and Z. Popovic, “Resistor emulation approach to low-power RF energy harvesting,” *IEEE Trans. Power Electron.*, vol. 23, no. 3, pp. 1494–1501, Mar. 2008.

[23] V. Marian, B. Allard, C. Vollaire, and J. Verdier, “Strategy for microwave energy harvesting from ambient field or a feeding source,” *IEEE Trans. Power Electron.*, vol. 27, no. 11, pp. 4481–4491, Nov. 2012.

[24] C. Song *et al.*, “A novel six-band dual CP rectenna using improved impedance matching technique for ambient RF energy harvesting,” *IEEE Trans. Antennas Propag.*, vol. 64, no. 7, pp. 3160–3171, Jul. 2016.

[25] H. Sun, Y.-X. Guo, M. He, and Z. Zhong, “Design of a high-efficiency 2.45-GHz rectenna for low-input-power energy harvesting,” *IEEE Antennas Wireless Propag. Lett.*, vol. 11, pp. 929–932, 2012.

[26] J. A. Hagerty, F. B. Helmbrecht, W. H. McCalpin, R. Zane, and Z. B. Popovic, “Recycling ambient microwave energy with broad-band rectenna arrays,” *IEEE Trans. Microw. Theory Techn.*, vol. 52, no. 3, pp. 1014–1024, Mar. 2004.

[27] Z. K. Ma and G. A. E. Vandenbosch, “Wideband harmonic rejection filtenna for wireless power transfer,” *IEEE Trans. Antennas Propag.*, vol. 62, no. 1, pp. 371–377, Oct. 2013.

[28] N. Shinohara and Y. Zhou, “Development of rectenna with high impedance and high Q antenna,” in *Proc. 2014 Asia–Pac. Microw. Conf.*, Nov. 2014, pp. 600–602.

[29] H. Miyagoshi, K. Noguchi, K. Itoh, and J. Ida, “High-impedance wideband folded dipole antenna for energy harvesting applications,” in *Proc. 2014 Int. Symp. Antennas Propag.*, Dec. 2014, pp. 601–602.

[30] H. Chu, Y.-X. Guo, and Z. Wang, “60-GHz LTCC wideband vertical offcenter dipole antenna and arrays,” *IEEE Trans. Antennas Propag.*, vol. 61, no. 1, pp. 153–161, Jan. 2013.

[31] R. Li, L. Pan, and Y. Cui, “A novel broadband circularly polarized antenna based on off-center-fed dipoles,” *IEEE Trans. Antennas Propag.*, vol. 63, no. 12, pp. 5296–5304, Dec. 2015.

[32] J. Belrose and P. Bouliane, “The off-center-fed dipole revisited: a broadband, multiband antenna,” *QST Mag.*, vol. 74, no. 8, pp. 28–34, 1990.

[33] J. Guo, H. Zhang, and X. Zhu, “Theoretical analysis of RF–DC conversion efficiency for class-F rectifiers,” *IEEE Trans. Microw. Theory Techn.*, vol. 62, no. 4, pp. 977–985, Apr. 2014.

[34] *Surface Mount Mixer and Detector Schottky Diodes*, *Data Sheet.* Skyworks Solutions, Inc., Woburn, MA, USA, 2013.

[35] S. Ladan, A. B. Guntupalli, and K. Wu, “A high-efficiency 24 GHz rectenna development towards millimeter-wave energy harvesting and wireless power transmission,” *IEEE Trans. Circuits Syst. I, Reg. Papers*, vol. 61, no. 12, pp. 3358–3366, Dec. 2014.

[36] J. D. Kraus and R. J. Marhefka, *Antennas: For All Applications*, 3rd ed. New York, NY, USA: McGraw-Hill, 2001.

[37] S. Schellkunoff, *Electromagnetic Waves*. New York, NY, USA: Van Nostrand, 1943.

[38] E. Spingola, “Multiband HF antennas, part 3, Windom and OCF dipole,” *Communicator*, vol. 13, no. 4, pp. 7–11, 2010.

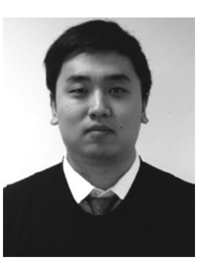

Chaoyun Song (S’16) received the B.Eng. (Hons.) degree in telecommunication engineering from Xi’an Jiaotong-Liverpool University, Suzhou, China, in 2012, and the M.Sc. degree with distinction in microelectronics and telecommunication in 2013 from the University of Liverpool, Liverpool, U.K., where he is currently working toward the Ph.D. degree in wireless communications and radio frequency engineering.

His current research interests include rectifying antennas, circular polarization antennas, power management circuits, wireless power transfer and energy harvesting, and wearable antennas.

Mr. Song has been a Regular Reviewer for the IEEE Transactions on Circuits and Systems I: Regular Papers, IEEE Transactions on Microwave Theory and Techinques, and IEEE Antennas and Wireless Propagation Letters.

Yi Huang (S’91–M’96–SM’06) received the D.Phil. degree in communications from the University of Oxford, Oxford, U.K., in 1994.

In 1995, he oined the Department of Electrical Engineering and Electronics, University of Liverpool, Liverpool, U.K., where he is currently a Full Professor in wireless engineering. He has published more than 200 refereed papers in leading international journals and conference proceedings, and is the principal author of the popular book *Antennas: From Theory to Practice* (Wiley, 2008). He has been conducting research in the areas of wireless communications, applied electromagnetics, radar, and antennas for the past 25 years.

Prof. Huang has been an Editor, an Associate Editor, or a Guest Editor of four international journals. He is at present the Editor-in-Chief of *Wireless Engineering and Technology*, an Associate Editor of the IEEE Antennas and Wireless Propagation Letters, a U.K. National Representative of the European COST-IC1102, a Fellow of the Institution of Engineering and Technology (IET), U.K., and an Executive Committee Member of the IET Electromagnetics PN.

Jiafeng Zhou received the B.Sc. degree in radio physics from Nanjing University, Nanjing, China, in 1997, and the Ph.D. degree from the University of Birmingham, Birmingham, U.K., in 2004. His Ph.D. research concerned high-temperature superconductor microwave filters.

Beginning in 1997, for two and a half years, he was with the National Meteorological Satellite Centre of China, Beijing, China, where he was involved in the development of communication systems for Chinese geostationary meteorological satellites. From 2004 to 2006, he was a Research Fellow with the University of Birmingham, where he was involved in phased arrays for reflector observing systems. Until 2013, he was with the Department of Electronic and Electrical Engineering, University of Bristol, Bristol, U.K., where he was involved in the development of highly efficient and linear amplifiers. He is currently with the Department of Electrical Engineering and Electronics, University of Liverpool, Liverpool, U.K. His current research interests include microwave power amplifiers, filters, electromagnetic energy harvesting, and wireless power transfer.

Paul Carter received the B.Sc. degree (Hons.) in physics from the University of Manchester, Manchester, U.K., in 1987, and the M.Sc. degree (Eng.) in microelectronic systems and telecommunications and the Ph.D. degree in electrical engineering and electronics from the University of Liverpool, Liverpool, U.K., in 1988 and 1991, respectively.

He is the President and the CEO of Global Wireless Solutions, Inc. (GWS), Dulles, VA, USA, a leading independent benchmarking solution vendor for the wireless industry. With more than 25 years of experience in the cellular network industry, he founded GWS to provide operators with access to in-depth, accurate network benchmarking, analysis, and testing. Prior to GWS, he directed business development and CDMA engineering efforts for LLC, the world’s largest independent wireless engineering company.

Sheng Yuan received the B.Eng. degree (first class) in microelectronics and telecommunication engineering and the Ph.D. degree in electrical engineering and electronics from the University of Liverpool, Liverpool, U.K., in 2012 and 2016, respectively.

He is currently with the Department of Intelligent Transportation Systems, Arup Group Limited, Newcastle, U.K. His research interests include wireless energy harvesting, ferromagnetic materials, indoor navigation systems, energy management circuits, wireless power transfer, radio-frequency identification, and intelligent transportation systems.

Qian Xu received the B.Eng. and M.Eng. degrees in electrical engineering and electronics from the Department of Electronics and Information, Northwestern Polytechnical University, Xi'an, China, in 2007 and 2010, respectively, and the Ph.D. degree in electrical engineering from the University of Liverpool, Liverpool, U.K., in 2016.

He is currently an Associate Professor in the College of Electronic and Information Engineering, Nanjing University of Aeronautics and Astronautics, Nanjing, China. He worked as an RF Engineer in Nanjing, China, in 2011, an Application Engineer at CST Company, Shanghai, China, in 2012, and a Research Assistant at the University of Liverpool in 2016. His research interests include statistical electromagnetics, reverberation chambers, computational electromagnetics, and anechoic chambers.

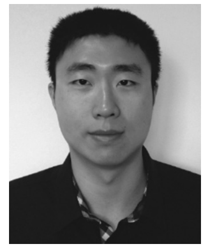

Zhouxiang Fei was born in Xi'an, China, in 1990. He received the B.Eng. degree in electronics and information engineering from Northwestern Polytechnical University, Xi'an, China, in 2012, and the M.Sc. degree with distinction in wireless communications from the University of Southampton, Southampton, U.K., in 2013. He is currently working toward the Ph.D. degree at the University of Liverpool, Liverpool, U.K.

His research interests include numerical and experimental studies of crosstalk in complex cable bundles, with a particular emphasis on considering parameter variability using efficient statistical approaches.

Mr. Fei received a student scholarship from the IEEE Electromagnetic Compatibility Society to attend the 2016 IEEE International Symposium on EMC, held in Ottawa, ON, Canada. He was also selected as a Best EMC Paper Finalist at the 2016 IEEE International Symposium on EMC.